Spread-Signature CDMA: Efficient Multiuser Communication in the Presence of Fading

Gregory W. Wornell, *Member, IEEE*

Abstract— **A new class of orthogonal code-division multiple-access (CDMA) systems is developed for efficient multiuser communication in environments subject to multipath fading phenomena. The key characteristic of these new systems, which we refer to as "spread-signature CDMA" systems, is that the associated signature sequences are significantly longer than the interval between symbols. Using this approach, the transmission of each symbol of each user is, in effect, spread over a wide temporal and spectral extent, which is efficiently exploited to combat the effects of fading. These systems generalize and improve on the spread-response precoding systems developed in [1].**

Both efficient signature sets and efficient receiver structures for such systems are developed. Several aspects of the performance of the resulting spread-signature CDMA systems are presented, including both the achievable bit-error rate characteristics and the effective capacity of such systems. The results suggest that spread-signature CDMA may be an attractive alternative to conventional CDMA in a variety of application scenarios.

Index Terms—**Multiuser communication, CDMA, wireless systems, Rayleigh fading channels, precoding.**

I. Introduction

SYSTEMS for efficiently coordinating communication among multiple users in multipath fading environments are important in a wide range of applications. Indeed, such systems are essential in proposed digital mobile radio communications, personal wireless systems, indoor wireless networks, and digital audio and television broadcasting systems. However, rapidly escalating demand for both wider availability of such services and increasingly sophisticated capabilities has put great pressure on the limited available bandwidth within the radio spectrum. Given such constraints, it is clear that the use of increasingly sophisticated signal processing in wireless modems will be critical to accommodate large numbers of services and users within the available spectrum.

In a comparison paper [1] we explored the use of a signal processing technique which we referred to as "spread-response precoding" for mitigating the effects of fading in single-user or frequency-division multiplexed data transmission systems used in multipath fading environments. From the perspective of the coded symbol stream, this precoding effectively transforms a fairly general Rayleigh fading channel into a nonfading, simple white marginally Gaussian additive noise channel with no intersymbol interference. By using such precoding to combat fading while reserving coding to combat only the remaining additive noise, substantial reductions in system complexity appear possible. Furthermore, although spread-response precoding represents a form of time diversity, it is efficient in the sense that it requires no additional power or bandwidth.

In this paper, we develop a natural generalization of the precoding concept for general multiuser communication problems in multipath fading environments. The result is a code-division multiple-access (CDMA) system in which, in effect, precoding is embedded directly into each user's signature sequence while maintaining orthogonality among users. We term the resulting system "spread-signature CDMA." These signature sequences have some very special characteristics as we will show, most notable of which is that their temporal extent significantly exceeds the intersymbol (baud) duration.

In a manner analogous to spread-response precoding, using such signature sets in multipath fading environments has the effect of transforming the collection of channels seen by the individual symbol streams from a collection of coupled Rayleigh fading channels into a uncorrelated collection of identical nonfading simple white marginally Gaussian additive noise channels. In essence, spread-signature CDMA converts various degradations due to fading, co-channel interference, and receiver noise into a single, comparatively more benign form of uncorrelated additive noise that is white and quasi-Gaussian.

Transformations of this type are, in general, highly desirable in multiuser systems; see, e.g., [2]. As we will see, spread-signature CDMA systems provide some important potential performance advantages over traditional CDMA systems. Furthermore, we will see that spread-signature CDMA systems achieve this benefit without requiring additional power or bandwidth, and are attractive in terms of computational complexity, robustness, and delay considerations.

Our model consists of a fairly general cellular multiple-access scenario in which each cell contains a single base station (sometimes referred to as a "cell site") and a number of mobiles (or, more generally, "subscribers"). We assume that both forward link (base-to-mobile) and reverse link (mobile-to-base) communication is required, but takes place on separate (i.e., noninterfering) channels. Between each

Manuscript received April 26, 1994; revised February 20, 1995. Part of this work was performed while the author was on leave from MIT at AT&T Bell Laboratories, Murray Hill, NJ 07974, during the 1992–1993 academic year. This work was supported in part by AT&T Bell Laboratories, by the Advanced Research Projects Agency monitored by ONR under Contract N00014-93-1-0686, and by the Air Force Office of Scientific Research under Grant AFOSR-91-0034.

The author is with the Department of Electrical Engineering and Computer Science and the Research Laboratory of Electronics, Massachusetts Institute of Technology, Cambridge, MA 02139 USA.

IEEE Log Number 9413762.

transmitter–receiver pair is a fairly general Rayleigh fading channel, which may be frequency-selective or nonselective.

The outline of the paper is as follows. In Section II, we develop the equivalent discrete-time baseband model for our multiuser system and some basic notation. In Section III we then develop a useful framework for characterizing the generalized orthogonal CDMA signature sets of interest in this work, and use this framework to develop an efficient family of spread-signature sets. Section IV develops some important aspects of spread-signature CDMA systems, ranging from transmission characteristics to channel-transformation properties of such systems. We then exploit these properties to develop efficient spread-signature CDMA receivers. Section V explores the potential performance of such optimized systems both in terms of capacity and bit-error rate characteristics, and Section VI contains some concluding remarks.

II. System Model

Consider a single cell of a multiple-access system, in which there are M users, all sharing a total fixed bandwidth $M\mathcal{W}_0$, so that $\mathcal{W}_0$ is the effective bandwidth per user. In the equivalent discrete-time baseband model for the system, the modulation process can be viewed as follows. The coded symbol stream of the mth user ($1 \leq m \leq M$), which we denote by $x_m[n]$, is modulated onto a unique signature sequence $h_m[n]$ to produce $y_m[n]$ which is transmitted within the total available bandwidth.

Conceptually, it is convenient to view the modulation process in two stages. As depicted in Fig. 1, these stages correspond to upsampling (i.e., zero insertion) by a factor M, followed by linear time-invariant filtering with the signature sequence, i.e.,

$$y_m[n] = \sum_k x_m[k] h_m[n - kM]. \tag{1}$$

The multiuser channel we consider, which is depicted in Fig. 2, is a rather general stationary Rayleigh fading environment with uncorrelated scattering. More specifically, $a_m[n;\, k]$ represents the zero-mean, complex-valued Gaussian kernel of the fading channel seen by that user. Hence, the sequence obtained at the receiver is

$$r[n] = \sum_m \sum_k a_m[n;\, k] y_m[n - k] + w[n] \tag{2}$$

where $w[n]$ is a zero-mean, complex-valued stationary white Gaussian sequence with variance[1]

$$E[|w[n]|^2] = \mathcal{N}_0 \mathcal{W}_0 \tag{3}$$

that is statistically independent of both the $a_m[n;\, k]$ and the $y_m[n]$. In general, the randomly time-varying kernels $a_m[n;\, k]$ capture the effects of multipath fading due to both fluctuations in the media and the relative motions of transmitters and receivers in the system. Meanwhile, $w[n]$ captures both receiver noise and any sources of cochannel interference not otherwise taken into account. We use $A_m(w;\, n]$ to denote the (stationary) time-variant frequency response corresponding to the mth channel.[2] Our notation for characterizing other aspects of this class of linear randomly time-varying systems is summarized for convenience in Appendix I.

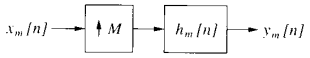

Fig. 1. Modulation of the mth user's coded symbol stream $x_m[n]$ onto a signature sequence $h_m[n]$ for transmission.

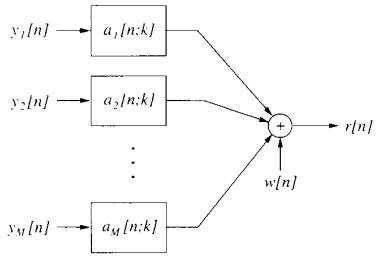

Fig. 2. General multiuser fading channel model, where $a_m[n;\, k]$ denotes the randomly time-varying linear kernel corresponding to the mth user.

Two special cases of this general channel model are of primary interest. The first, corresponding to base-to-mobile transmission, is referred to as the forward link. In this case, the messages to the individual mobiles are multiplexed together before being broadcast over the channel. From the perspective of a particular receiver all messages are transmitted through the same channel, i.e.,

$$a_1[n;\, k] = a_2[n;\, k] = \cdots = a_M[n;\, k] \triangleq a[n;\, k]. \tag{4}$$

The second case, corresponding to mobile-to-base transmission, is referred to as the reverse link. In this case, the messages are transmitted through separate channels to the base station. With reasonable physical separation among mobiles, as we will assume, the kernels of the individual mobile-to-base channels may be modeled as mutually independent. We shall further assume that no base-to-mobile feedback channel is available to provide synchronization information to the mobiles. Accordingly, the kernels $a_m[n;\, k]$ in our model capture the effects of both multipath fading and asynchronism among users.

Finally, we make the reasonable assumption that, in both forward and reverse link cases, while the transmitters have no knowledge of the channel kernels $a_m[n;\, k]$ or their statistics, these parameters are known—or, more typically, can be reliably measured—at the corresponding receivers in the system.

[1] Note that, for convenience, in our equivalent model the channel parameters are bandwidth-normalized, i.e., the statistics of both $a_m[n;\, k]$ and $w[n]$ are independent of the bandwidth parameter M. To maintain the proper dependence of signal-to-noise ratio on M, we therefore bandwidth-normalize the transmitted power as well. Indeed, as we will establish in Section IV-A, when the coded stream $x_m[n]$ has power $\mathcal{E}_m$, the transmitted stream $y_m[n]$ has power $\mathcal{E}_m/M$.

[2] We adopt the useful convention of using parenthesis $(\cdot)$ to denote continuous-valued arguments and brackets $[\cdot]$ to denote discrete-valued arguments. For functions of two arguments where the first is continuous and the second is discrete (as in the case of time-variant frequency responses) we use the convenient mixed notation $(\cdot;\, \cdot]$. The notation $[\cdot;\, \cdot)$ is used in a similar manner.

III. Orthogonal Multiuser Modulation

In traditional CDMA systems, the signature sequences $h_m[n]$ used in the modulation (1) have length equal to the upsampling rate or intersymbol period M. In this way, the signatures are used in a nonoverlapping manner. However, in this section we consider signatures of arbitrary length N. When $N > M$, the resulting sequences have valuable partial response characteristics akin to those of spread-response precoding, and we refer to these sequences as "spread-signature" sequences.

A useful mathematical framework for representing such signature sets arises out of multirate system theory [3], as we now show. To begin, we first express the signature set as the vector sequence, i.e.,[3]

$$\boldsymbol{h}[n] = [h_1[n] h_2[n] \cdots h_M[n]]^T \tag{5}$$

and, for convenience, let us restrict our attention to real-valued signature sets. When each of the component signatures $h_m[n]$ has only finitely many nonzero values, we shall refer to the signature set as having *finite spread.* Specifically, when

$$\boldsymbol{h}[n] = \boldsymbol{0}, \quad n < 0,\ n \geq N$$

we say that the signature set has *temporal spread* N.

Although the theory can accommodate more general classes of signature sets, we restrict our attention to those satisfying certain convenient orthogonality conditions, which facilitate both analysis and implementation. Specifically, we require that the signature sequences together with all translates by integer multiple of M constitute an orthonormal set, i.e.,[4]

$$\sum_k \boldsymbol{h}[k - nM]\boldsymbol{h}^T[k - mM] = \delta[n - m]\boldsymbol{I} \tag{6}$$

where $\boldsymbol{I}$ denotes the identity matrix of appropriate size, and where $\delta[n]$ denotes the unit sample, viz.,

$$\delta[n] \triangleq \begin{cases} i, & n = 0 \\ 0, & \text{otherwise} \end{cases}. \tag{7}$$

In turn, the corresponding completeness condition for this orthonormal set can be expressed as

$$\sum_k \boldsymbol{h}^T[n - kM]\boldsymbol{h}[m - kM] = \sum_{k,\,i} h_i[n - kM] h_i[m - kM] = \delta[n - m] \tag{8}$$

and, in fact, (8) can be interpreted as a special instance of Mercer's Theorem [4].

It is important to emphasize that orthonormal signature sets, i.e., sets satisfying (6) and (8), correspond to lossless systems. As a result, demodulation in the absence of distortion is particularly simple. To illustrate, if the input symbol streams are $x_m[n]$ and the superimposed output is the sequence $y[n]$, i.e., via (1)

$$y[n] = \sum_{m=0}^{M-1} y_m[n] = \sum_{m,\,k} h_m[n - Mk] x_m[k] \tag{9}$$

then the sequences $x_m[n]$ can be reconstructed from $y[n]$ via

$$x_m[n] = \sum_k h_m[k - nM] y[k]. \tag{10}$$

As we shall see, the discrete-time matched-filter and downsample operation (10) is also a key component of the demodulation process when distortion is present as well.

For $M \geq 2$, there is a rich collection of signature sets satisfying (6) and (8), even when we restrict our attention to signatures with finite spread. For $M = 1$, however, the modulation process (1) is equivalent to prefiltering with a linear time-invariant filter whose unit-sample response is the signature sequence $h_1[n]$. In this case, which was extensively developed in [1], the condition (6) is equivalent to requiring that $h_1[n]$ be an allpass filter, and it is well-known that nontrivial finite-length allpass filters do not exist.

Several aspects of orthogonal signature sets are more conveniently viewed in the frequency domain. Accordingly, we express the set of Fourier transforms corresponding to (5) in the form

$$\boldsymbol{H}(\omega) = \int_{-\infty}^{+\infty} \boldsymbol{h}[n] e^{-j\omega n}\, d\omega \triangleq [H_1(\omega)\ H_2(\omega) \cdots H_M(\omega)]^T. \tag{11}$$

For example, the orthogonality properties (6) and (8) are frequently more conveniently viewed in the frequency domain—as an illustration, (8) is equivalent to[5]

$$\boldsymbol{H}^\dagger(\omega)\boldsymbol{H}(\omega) = \sum_k |H_k(\omega)|^2 = M \tag{12}$$

which is sometimes referred to as a (power) complementarity condition.

More importantly, the frequency-domain representation (11) leads to the efficient factorization

$$\boldsymbol{H}(\omega) = \boldsymbol{Q}(M\omega)\boldsymbol{\Delta}(\omega) \tag{13}$$

where $\boldsymbol{Q}(\omega)$ is a square matrix and $\boldsymbol{\Delta}(\omega)$ is the Fourier transform of the delay chain of order M, i.e.

$$\boldsymbol{\delta}[n] = [\delta[n]\ \delta[n-1] \cdots \delta[n - M + 1]]^T \tag{14}$$

whence

$$\boldsymbol{\Delta}(\omega) = [1\ e^{-j\omega} \cdots e^{j\omega(M-1)}]^T. \tag{15}$$

The decomposition (13) is referred to as the *polyphase* representation of the set, and $\boldsymbol{Q}(\omega)$ is termed the associated polyphase matrix. As is true for multirate systems in general [3], polyphase representations of signature sequences are not only conceptually useful, but lead to computationally efficient modem implementations as well.

For specifically orthonormal signature sets, the associated polyphase matrix satisfies the special property

$$\boldsymbol{Q}(\omega)\boldsymbol{Q}^\dagger(\omega) = \boldsymbol{I} \tag{16}$$

and we remark that matrices satisfying (16) are termed *paraunitary*. Furthermore, it is straightforward to verify that $\boldsymbol{Q}(\omega)$ is

[3] The superscript ^{T} denotes transposition.

[4] Note that (6) directly incorporates the natural requirement that each signature sequence $h_m[n]$ have unit energy.

[5] The superscript † denotes the conjugate-transpose operation.

independent of ω if and only if the signature set is *not* spread (i.e., $N = M$).

The polyphase matrices associated with some familiar orthogonal signature sets provide useful insight. For example, the polyphase matrix corresponding to time-division multiple-access (TDMA) systems is

$$\boldsymbol{Q}(\omega) = \boldsymbol{I}$$

while that corresponding to ideal frequency-division multiple-access (FDMA) systems has (k, l)th element[6]

$$[\boldsymbol{Q}(\omega)]_{k,l} = e^{j(\omega - 2\pi k)l/M}, \qquad 0 \le \omega \le \pi.$$

In contrast, for discrete Fourier transform (DFT) multiplexing, $\boldsymbol{Q}(\omega)$ is the DFT matrix, i.e.

$$[\boldsymbol{Q}(\omega)]_{k,l} = e^{-j2\pi kl/M}.$$

For Hadamard sequence based CDMA systems, for which we will develop a powerful generalization in Section III-A, we have

$$\boldsymbol{Q}(\omega) = \boldsymbol{\Xi}$$

where $\boldsymbol{\Xi}$ is the Hadamard matrix of appropriate dimension. Recall that the Hadamard matrix of dimension M, viz., $\boldsymbol{\Xi}_M$, where M is a power of two, is defined recursively: for $M = 2, 4, \cdots$

$$\boldsymbol{\Xi}_M = \frac{1}{\sqrt{2}}\begin{bmatrix} \boldsymbol{\Xi}_{M/2} & \boldsymbol{\Xi}_{M/2} \\ \boldsymbol{\Xi}_{M/1} & -\boldsymbol{\Xi}_{M/2} \end{bmatrix}$$

where $\boldsymbol{\Xi}_1 = 1$.

CDMA system designers are frequently interested in the auto- and crosscorrelation characteristics of the signature sequences. Indeed, the autocorrelation characteristics generally affect, for example, the ability of a receiver to synchronize to the transmission, while the cross-correlation characteristics generally affect the degree and nature of co-channel interference. Ideally, therefore, one would like the autocorrelation of each signature $h_k[n]$ to satisfy[7]

$$h_k[n] * h_k[-n] \approx \delta[n] \tag{17}$$

and the crosscorrelation between distinct signatures $h_k[n]$ and $h_l[n]$ to satisfy

$$h_k[n] * h_l[-n] \approx 0, \qquad k \ne l. \tag{18}$$

It is well-known that (17) and (18) are conflicting objectives for traditional signature sets (see, e.g., Welch [5] or Sarwate and Pursley [6]). In fact, this is also true for spread-signature sets. To see this, let us define quadratic auto- or crosscorrelation merit factors which penalize deviations from (17) and (18), respectively. Specifically, analogous to the merit factors defined by Golay [7], let

$$1/\mathcal{L}_{kl}^h = \frac{1}{2\pi}\int_{-\pi}^{\pi} [|H_k(\omega)H_l^*(\omega)| - \delta[k-l]]^2\, d\omega. \tag{19}$$

[6]Note that $\boldsymbol{Q}(\omega)$ is both conjugate symmetric, i.e., $\boldsymbol{Q}^*(\omega) = \boldsymbol{Q}(-\omega)$, and 2π-periodic. The superscript * denotes complex conjugation.

[7]The operator $*$ denotes convolution.

Then, using (12), it is straightforward to verify that, for any $M \ge 2$

$$\begin{aligned}\frac{1}{M^2}\sum_{k,l}\frac{1}{\mathcal{L}_{kl}^h} &= \frac{1}{2\pi M^2}\int_{-\pi}^{\pi}\left[\sum_k (|H_k(\omega)|^4 - 2|H_k(\omega)|^2 + 1)\right. \\ &\quad \left. + \sum_{k,\, l\ne k} (|H_k(\omega)|^2|H_l(\omega)|^2)\right] d\omega \\ &= \frac{1}{2\pi}\int_{-\pi}^{\pi}\frac{(M-1)}{M}d\omega = \frac{(M-1)}{M}. \end{aligned} \tag{20}$$

Hence, from (20), we see that good autocorrelation characteristics can only be obtained at the expense of crosscorrelation characteristics, and *vice versa*. At one extreme the trivial signature set corresponding to TDMA systems has perfect autocorrelation characteristics, but the worst possible cross-correlation characteristics,[8] i.e.

$$\mathcal{L}_{kl}^h = \begin{cases} \infty, & k = l \\ 1, & k \ne l \end{cases}.$$

At the opposite extreme we have the signature set corresponding to ideal FDMA systems. This set has perfect crosscorrelation characteristics but poor autocorrelation characteristics; in particular

$$\mathcal{L}_{kl}^h = \begin{cases} 1/(M-1), & k = l \\ \infty, & k \ne l \end{cases}.$$

In practical CDMA systems, a compromise between these extremes is generally sought.

The auto- and crosscorrelation characteristics constitute only one of the important issues in the design of good spread signature sets. For example, it is also important that the signature sets we develop are effective in spreading the transmission of each symbol of a user's transmission over a large range of time samples in order to mitigate the effects of fading. This is, of course, analogous to the objectives of spread-response precoding as developed in [1]. Accordingly, we define a dispersion factor $\mathcal{D}_h$ which measures a signature set's spreading capability via

$$\frac{1}{\mathcal{D}_h} = \frac{1}{M}\sum_m \frac{1}{\mathcal{D}_{h_m}} \tag{21}$$

where $\mathcal{D}_{h_m}$ represents the dispersion in the sequence $h_m[n]$, i.e., consistent with [1]

$$\mathcal{D}_{h_m} = \left(\sum_m h_m^4[n]\right)^{-1}. \tag{22}$$

Note from (21) that, as we would expect from any reasonable definition of dispersion, the set has perfect spreading, i.e., $\mathcal{D}_h \to \infty$, if and only if every signature in the set is perfectly spread, i.e., $\mathcal{D}_{h_m} \to \infty$ for every $1 \le m \le M$.

[8]In fact, as can be verified from (19) and (20), this is true for any orthogonal signature set whose sequences have allpass Fourier transforms.

Important insights are obtained by examining what values $\mathcal{D}_h$ can take. It is straightforward to verify, for instance, that for all orthonormal signature sets

$$\mathcal{D}_h \geq 1 \tag{23}$$

and that this bound is attained when $\boldsymbol{h}[n]$ is the TDMA signature set. More importantly, at another extreme we have, for finite-spread signature sets with temporal spread N

$$\mathcal{D}_h \leq N \tag{24}$$

with equality precisely when, for each $1 \leq m \leq M$

$$|h_m[n]| = 1/\sqrt{N}, \qquad 0 \leq n \leq N-1.$$

Hence, for finite-spread signature sets, maximum dispersion is achieved when the signature sequences are antipodal (binary-valued). For this reason, we refer to the corresponding signature sets as "maximally spread." Note, too, that because they are discrete-valued, maximally spread signature sets are especially attractive in terms of computational efficiency and numerical stability.

As another important design issue, it will also be important that the spread-signature sets we use possess what we refer to as a good "partitioning" characteristics. In particular, as we will see, good partitioning results in more uniform distribution of cochannel interference among users in the system. To develop this concept, we define the following modified correlation function:

$$\Theta_{h_i}[n, m] = \sum_k h_i[n - Mk]h_i[m - Mk] \tag{25}$$

which corresponds to correlating $h_i[n]$ with a version of $h_i[n]$ in which all but every Mth sample is replaced with zero. While the complementarity condition (8) directly implies that

$$\sum_i \Theta_{h_i}[n, m] = \delta[n - m] \tag{26}$$

this condition says nothing about the properties of each of the M terms in the summation of (26). However, as will become apparent in Section IV, the set has good partitioning characteristics when the unit sample in (26) is, in some sense, distributed uniformly among the M modified correlation functions.

To make the notion of good partitioning characteristics more precise, we let

$$\tilde{\Theta}_{h_i}[n, m] = \Theta_{h_i}[n, m] - \frac{1}{M}\delta[n - m] \tag{27}$$

denote the deviation from ideal partitioning in each component. It is straightforward to show that $\tilde{\Theta}_{h_i}[n, m]$ is the following symmetry, periodicity, and finite-energy characteristics:

$$\tilde{\Theta}_{h_i}[n, m] = \tilde{\Theta}_{h_i}[m, n] \tag{28a}$$

$$\tilde{\Theta}_{h_i}[n, m] = \tilde{\Theta}_{h_i}[n + kM, m + kM], \qquad \text{any } k \tag{28b}$$

and

$$1/M^2 \leq \sum_n \tilde{\Theta}^2_{h_i}[n, m] \leq (1 - 1/M)^2. \tag{28c}$$

A signature set has asymptotically perfect partitioning if $\tilde{\Theta}_{h_i}[n, m]$ can be made arbitrarily small using sufficiently long signatures. Accordingly, we define the following *partitioning factor:*

$$\frac{1}{\chi_h} = \frac{1}{M}\sum_i \frac{1}{\chi_{h_i}} \tag{29}$$

where

$$\frac{1}{\chi_{h_i}} = \sup_m \sum_n \tilde{\Theta}^4_{h_i}[n, m] \tag{30}$$

and note that good partitioning corresponds to large partitioning factors, and *vice versa.* It is important to note, however, that signature sets with good dispersion factors do not necessarily have good partitioning characteristics.[9] Nevertheless, we emphasize that we shall be primarily interested in signature sets which have both good dispersion and good partitioning characteristics.

A. An Optimum Class of Spread-Signature Sets

In this section, we develop a family of orthogonal signature sets that are optimal in the sense of being maximally spread, i.e., having the best dispersion characteristics for a given length (or, equivalently, delay) constraint. As we discussed earlier, the maximally spread condition is achieved precisely when the signature sequences are binary-valued. The signatures we construct are conveniently obtained out of a powerful paraunitary generalization of the Hadamard matrix, and have a computationally efficient recursive synthesis that is attractive in terms of modem implementation.

Our construction is based on the polyphase decomposition of a signature set (13). In particular, we rephrase the problem of designing a suitable orthogonal signature set $\boldsymbol{H}(\omega)$ into problem of designing a suitable paraunitary polyphase matrix $\boldsymbol{Q}(\omega)$. Thus requiring that the desired $\boldsymbol{H}(\omega)$ correspond to a maximally spread signature set is equivalent to requiring that the polyphase matrix sequence $\boldsymbol{q}[n]$ whose transform is $\boldsymbol{Q}(\omega)$ be binary-valued.

We begin by observing that the Hadamard matrix $\boldsymbol{\Xi}$ is one matrix satisfying these properties. Accordingly, we let our zeroth-order polyphase matrix be[10]

$$\boldsymbol{Q}^{(0)}(\omega) = \boldsymbol{\Xi} \tag{31}$$

and note that the spread of the corresponding signature set is $N = M$.

[9] To verify this, it suffices to note that from any orthogonal signature set $h_m[n]$, we can construct a new orthogonal signature set $g_m[n]$ via

$$g_m[n] = \sum_k e_m[k]h_m[n - kM]$$

where the $e_m[n]$ are any set of nontrivial lossless (allpass) filters. However, while this new system generally has greater dispersion $\mathcal{D}_g > \mathcal{D}_h$, it is straightforward to show that the partitioning factor is unchanged, i.e., $\chi_g = \chi_h$.

[10] For convenience, we restrict our attention to orders M for which Hadamard matrices exist. These include, for example, all integers M that are powers of two.

To obtain signature sets for which $N > M$, we exploit a recursion that preserves the binary sequence requirement; specifically, we let

$$\boldsymbol{Q}^{(i)}(\omega) = \boldsymbol{\Xi}\boldsymbol{\Lambda}(M^{i-1}\omega)\boldsymbol{Q}^{(i-1)}(\omega), \qquad i = 1, 2, \cdots \quad (32)$$

where $\boldsymbol{\Lambda}(\omega)$ is the diagonal delay matrix whose diagonal is constructed from the elements of $\boldsymbol{\Delta}(\omega)$, i.e., with $\boldsymbol{\Delta}(\omega)$ as defined in (15),

$$\boldsymbol{\Lambda}(\omega) = \text{diag } \boldsymbol{\Delta}(\omega).$$

We see immediately that the paraunitary property (16) is preserved by the recursion (32) because the product of paraunitary matrices is also paraunitary. It is similarly straightforward to verify that the recursion (32) preserves the binary sequence property—indeed, in the time domain one can interpret (32) and (31) as implementing a succession of simple sequence concatenations initiated with Hadamard sequences.

Using (13), we can also express the recursion (32) directly in terms of the signature set vector Fourier transform; specifically, we have, for $i = 1, 2, \cdots$

$$\boldsymbol{H}^{(i)}(\omega) = \boldsymbol{\Xi}\boldsymbol{\Lambda}(M^{i}\omega)\boldsymbol{H}^{(i-1)}(\omega). \quad (33)$$

From (33) we can verify that the spread of the signature set grows by a factor of M with each application of the recursion, so that, in particular, $\boldsymbol{H}^{(i)}(\omega)$ has spread $N = M^{i+1}$ for $i = 0, 1, 2, \cdots$. For convenience, several sets of signature sequences obtained by the recursion (32) with (31), and corresponding to different values of M and N, are tabulated in Appendix II.

As a historical aside, it is interesting to note that orthogonal systems of the type constructed in this section have been reinvented numerous times over the last several decades, particularly for the case corresponding to $M = 2$. However, it would appear that this work is the first to attempt to exploit such systems in multiuser communication problems.

Using a variety of constructions, such systems emerged independently in a variety of unrelated communities within mathematics, physics, and engineering. Work within the engineering community dates traced back to 1950 when Golay constructed pairs of pseudorandom sequences which he referred to as "complementary sequences" [8], [9]. These sequences—now frequently referred to as Golay sequences—were defined as binary-valued sequences satisfying the frequency-domain complementarity condition (12) for $M = 2$.[11] These Golay sequences have subsequently been explored extensively, though the focus has been primarily on issues of existence of such pairs for various values of N; see, e.g., [10] and [11].

From (12) it is apparent that binary-valued orthogonal sequences are a subset of complementary sequences. However, more importantly, complementary sequences are also useful in the construction of orthogonal sequences, which both Golay and Turyn [12], and later Taki, *et al.* [13] observed in the case[12] $M = 2$. The corresponding generalizations for $M > 2$ appear in, e.g., Tseng and Liu [14].

Within the mathematics community, binary-valued, pseudorandom, orthogonal sequence pairs (and, in particular, a time-domain version of the recursion (33) for $M = 2$) were also discovered independently by both Shapiro [15] and, later, Rudin [16]. As a result, the frequency-domain representations for such sequences are sometimes referred to as Rudin–Shapiro polynomials.

As discussed in, e.g., Odlyzko [17], several useful properties of such sequences, as well as their connections to other families of binary pseudorandom sequences, have been developed. For example, the asymptotic auto- and crosscorrelation characteristics of our maximally spread orthogonal signature sets for the case $M = 2$ follow immediately from the results of Newman and Byrnes [18]. In particular, we have that

$$\mathcal{L}^h_{kk} \to 3, \qquad N \to \infty \quad (35)$$

which, using (20), implies that for $k \neq l$

$$\mathcal{L}^h_{kl} \to 3/2, \qquad N \to \infty. \quad (36)$$

Based on earlier discussion in Section III, (35) and (36) suggest that our maximally spread signature sets are localized in neither time nor frequency. In fact, not only is this the case, but such strong spreading in *both* time and frequency is critical to good performance in our intended application. Furthermore, in addition to their good spreading characteristics, our maximally spread signature sets have good asymptotic partitioning characteristics as well; specifically, $\chi_h \to \infty$ as $N \to \infty$.

IV. System Characteristics

In this section, we develop the key characteristics of spread-signature CDMA systems, and then apply these results in developing efficient receivers for such systems. We begin with a general discussion of transmission characteristics.

A. Transmission Characteristics

Spread-signature CDMA systems give rise to transmissions with some rather special spectral and temporal characteristics, only some of which are shared by conventional CDMA systems. To illustrate the spectral features, we begin by observing from (1) that, provided the coded symbol stream of the mth user is stationary, the corresponding transmitted stream is cyclostationary with a time-averaged power spectrum given by

$$S_{y_m}(\omega) = |H_m(\omega)|^2 S_{x_m}(M\omega)/M$$

where $S_{x_m}(\omega)$ is the power spectrum of the coded symbols of the mth user. When $x_m[n]$ consists of uncorrelated symbols of energy $\mathcal{E}_m$, as we shall generally assume in practice, the

[11] As such, there is a natural correspondence between such complementary pairs and power complementary filters as developed in the multirate signal processing literature [3].

[12] To see this, it suffices to verify using (16) with (12) that

$$\boldsymbol{Q}(\omega) = \begin{bmatrix} A(\omega) & B(\omega) \\ B^*(\omega) & -A^*(\omega) \end{bmatrix} \quad (34)$$

is a paraunitary matrix whenever the corresponding sequences $a[n]$ and $b[n]$ constitute a complementary pair.

transmitted power spectrum associated with the mth user further simplifies to

$$S_{y_m}(\omega) = |H_m(\omega)|^2 \mathcal{E}_m / M. \tag{37}$$

From (37) several observations can be made. First, we immediately note that since $H_m(\omega)$ has unit energy, the total transmitted power in this case is $\mathcal{E}_m/M$. When compared with (3) we see that this appropriately results in a signal-to-noise ratio (SNR) that decreases inversely with system bandwidth.

We also note from (37) that, in general, the transmitted power spectrum, is not, strictly speaking, white. However, when the maximally spread signature sets of Section III-A are used, the transmitted power spectrum is broadband and, in a particular sense, asymptotically white. More specifically, as $N \to \infty$, each $H_m(\omega)$ "converges" to a highly irregular function whose energy is *effectively* uniformly distributed over frequency. Furthermore, the transmitted spectrum corresponding to forward link transmission is typically truly white. Indeed, when the component coded symbol streams are mutually uncorrelated and of equal energy $\mathcal{E}_m = \mathcal{E}$, it is straightforward to verify using (12) that the aggregate transmitted power spectrum is

$$S_y(\omega) = \mathcal{E} \tag{38}$$

where $y[n]$ is the aggregate transmission, i.e.

$$y[n] = \sum_m y_m[n]. \tag{39}$$

The temporal characteristics of spread-signature CDMA transmissions are noteworthy as well. In traditional CDMA systems the individual (baseband) transmissions are generally binary-valued. However, in spread-signature CDMA systems, although the signature sequences and coded streams may be binary-valued, (if, e.g., the signature sequences of Section III-A are used), the transmitted streams generated via the modulation (1) generally are not. This is, of course, a consequence of the overlap between modulated symbols than invariably results from choosing signature sequence lengths N that exceed the intersymbol epoch M. In fact, as $N \to \infty$, a simple Central Limit Theorem argument suggests that each $y_m[n]$ is a marginally Gaussian process.

This quasi-Gaussian behavior is generally rather appealing from the point of view of certain transmission security and capacity considerations. However, it is important to point out that, as was true in the case of spread-response precoding systems, these characteristics also pose significant engineering challenges in terms of managing peak-to-average power and receiver synchronization requirements. While such issues certainly warrant further investigation, they are beyond the scope of the present paper.

B. Receiver Characteristics and Design

In Section IV-A we explored the transmission characteristics of spread-signature CDMA by examining what the coded symbol streams look like (after modulation) from the perspective of the channel. In this section, we develop efficient receivers for such systems by examining what the channel looks like from the perspective of the coded symbol stream (before modulation).

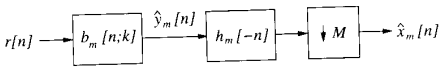

Fig. 3. Receiver structure for extracting the symbol stream of the mth user. The first stage is equalization, producing $\hat{y}_m[n]$, while the second stage is demodulation, producing $\hat{x}_m[n]$. A final stage (not shown) is decoding.

We begin by observing that what the coded symbol stream, in effect, "sees" is the cumulative effect of modulation, followed by distortion introduced by the channel, followed by processing performed at the receiver. Accordingly, we refer to what the coded symbol stream sees, then, as the "composite channel."

Before we explore the key properties of this composite channel, we must first develop an appropriate receiver structure for these systems. In general, the receiver processing required to recover the mth transmitted message is comprised of three stages. First, the received data $r[n]$ are equalized according to

$$\hat{y}_m[n] = \sum_k b_m[n; k] r[n-k]. \tag{40}$$

As is apparent from (40) and depicted in Fig. 3, the corresponding equalizer is, in general, a linear time-varying filter whose kernel we denote by $b_m[n; k]$. Because the fading channel coefficients and statistics are assumed to be available to the receiver, the equalizer kernel $b_m[\cdot; \cdot]$ is generally a function of all the channel kernels $a_k[\cdot; \cdot]$, $k = 1, 2, \cdots M$, although the dependence is often simpler in certain special cases of interest.

In the second stage, also depicted in Fig. 3, the equalized data are demodulated from the corresponding signature sequence, viz.,

$$\hat{x}_m[n] = \sum_k \hat{y}_m[k] h_m[k - Mn]. \tag{41}$$

This is conveniently interpreted as a discrete-time matched-filter and downsample operation.

Finally, the last stage of the message recovery, which is not depicted in Fig. 3, consists of decoding the demodulated stream $\hat{x}_m[n]$ (using, for example, maximum-likelihood methods). It is important to point out, however, that while we will not consider the actual implementation of the decoder in this paper, we will discuss in Section V what kinds of coding and decoding strategies are appropriate for spread-signature CDMA, and their effect on system performance.

The composite system consisting of modulation, the channel, equalization, and demodulation has some appealing characteristics provided the channel, and, in turn, the corresponding equalizers, have some reasonable ergodicity properties. In effect, these ergodic properties are required to ensure that spreading the transmission of each symbol over a sufficiently long time interval by modulation allows these symbols to see the average characteristics of the fading channel—i.e., that the time averaging implicit in the modulation is equivalent to ensemble averaging. The following technical definition will prove to be sufficient for our purposes.

Definition 1: Let $f_j[n;\, k]$ be the kernels of a family of linear systems, and define

$$\tilde{f}_j[n;\, k] = f_j[n;\, k] - E[f_j[n;\, k]]. \tag{42}$$

Furthermore, let

$$d_j^{j'}[n,\, m;\, k,\, l] = \tilde{f}_j[n;\, k]\tilde{f}_{j'}^{*}[m;\, l] \tag{43}$$

and define

$$\tilde{d}_j^{j'}[n,\, m;\, k,\, l] = d_j^{j'}[n,\, m;\, k,\, l] - E[d_j^{j'}[n,\, m;\, k,\, l]]. \tag{44}$$

Then the family $f_j[n;\, k]$ is *admissibly ergodic* if the following conditions are satisfied:

$$E[f_j[n;\, k]] = E[F_j]\delta[k] \tag{45a}$$

$$E[\tilde{f}_j[n;\, k]\tilde{f}_{j'}^{*}[m;\, l]] = R_j^{j'}[n-m;\, k]\delta[k-l] \tag{45b}$$

$$E[\tilde{d}_j^{j'}[n,\, m;\, k,\, l]\ \tilde{d}_j^{j'*}[n',\, m';\, k',\, l']] = T_j^{j'}[n-m,\, n'-m',\, n-n';\, k,\, l,\, k',\, l'] \tag{45c}$$

$$S_{R_j^{j'}} = \sum_n \sum_k |R_j^{j'}[n;\, k]| < \infty \tag{45d}$$

$$S_{T_j^{j'}} = \sum_{\substack{n_1,\, n_2\\ n_3}} \sum_{\substack{k_1,\, k_2\\ k_3,\, k_4}} |T_j^{j'}[n_1,\, n_2,\, n_3;\, k_1,\, k_2,\, k_3,\, k_4]| < \infty. \tag{45e}$$

Definition 1, in fact, represents a straightforward generalization of the corresponding definition in [1]. In particular, conditions (45a), (45b), and (45c) are essentially stationarity constraints, while (45d) and (45e) are ergodicity constraints. Note, too, that for convenience we have omitted specification of the frequency ω and time n from $E[F_j(\omega;\, n)]$ in (45a) due to stationarity.

The key properties of the composite channels, which we now develop, represent a natural generalization of those developed for single-user systems in [1]. In particular, we show that subject to only relatively mild ergodicity constraints, the use of spread-signature modulation with sufficiently long signatures leads to composite channels that are effectively a collection of uncorrelated additive white-noise channels, each of which is not only free of fading, but has no intersymbol interference. In developing our detailed results, we consider the forward-link and reverse-link systems separately since there are some fundamental differences in behavior.

1) The Forward Link: The characteristics of the composite system for the forward link are summarized in the following theorem. A proof is provided in Appendix III.

Theorem 1 (Forward Link): Let $x_m[n]$ be mutually uncorrelated sequences of zero-mean, uncorrelated symbols, each with energy $\mathcal{E}_m$, and let $a_m[n;\, k]$ and $w[n]$ be as defined in (2) and (4). Furthermore, let the common equalizer be

$$b_1[n;\, k] = b_2[n;\, k] = \cdots = b_m[n;\, k] \triangleq b[n;\, k]$$

and let $c[n;\, k]$ denote the kernel of the linear system formed by cascading the channel whose kernel is $a[n;\, k]$, with the equalizer whose kernel is $b[n;\, k]$, i.e.

$$c[n;\, k] = \sum_l b[n;\, l]a[n-l;\, k-l]. \tag{46}$$

Finally, suppose the $c[n;\, k]$ and $b[n;\, k]$ are both admissibly ergodic kernels in the sense of Definition 1, and let $\hat{x}_m[n]$ be defined via (41) and (40). Then, as $\mathcal{D}_h \to \infty$ (infinite dispersion) and $\chi_h \to \infty$ (perfect partitioning[13]), we have, for each n,[14]

$$\hat{x}_m[n] \overset{\text{m.s.}}{\to} E[C]x_m[n] + v_m[n] \tag{47}$$

where the $v_m[n]$ are mutually uncorrelated, zero-mean, complex-valued, marginally Gaussian white-noise sequences that are uncorrelated with the input symbol sequences $x_m[n]$. Furthermore, the variance of the noise $v_m[n]$ is independent of both m and n, and is given by

$$\operatorname{var} v_m[n] = \mathcal{N}_0\mathcal{W}_0 E[|B|^2] + \operatorname{var}[C]\overline{\mathcal{E}} \tag{48}$$

where

$$\overline{\mathcal{E}} = \frac{1}{M}\sum_{k=1}^{M} \mathcal{E}_k \tag{49}$$

is the average transmitted power. In both (47) and (48) we have, for convenience, again omitted specification of the time sample n and frequency ω corresponding to B and C due to stationarity.

While we postpone more general remarks until Section IV-B3, we emphasize that Theorem 1 implies that the composite forward-link channels are asymptotically mutually uncorrelated, identical, nonfading, quasi-Gaussian channels with no intersymbol interference. Moreover, from Theorem 1 we also note that the SNR on the mth of these composite channels is

$$\gamma_m = \frac{\mathcal{E}_m |E[C]|^2}{\mathcal{N}_0\mathcal{W}_0 E[|B|^2] + \overline{\mathcal{E}} \operatorname{var}[C]}. \tag{50}$$

The design of a suitable equalizer for the receiver in this case is straightforward. In particular, for sufficiently slow fading we have

$$C(\omega;\, n] \approx A(\omega;\, n]B(\omega;\, n]$$

so that (50) becomes

$$\gamma_m = \frac{\mathcal{E}_m}{\overline{\mathcal{E}}}\left[\frac{|E[AB]|^2}{(\mathcal{N}_0\mathcal{W}_0/\overline{\mathcal{E}})E[|B|^2] + \operatorname{var}[AB]}\right]. \tag{51}$$

Then, recognizing that the term in brackets in (51) is identical in form for an SNR expression that was maximized in [1], we immediately deduce that (50) is maximized when

$$B(\omega;\, n] \propto \frac{A^*(\omega;\, n]}{1+\overline{\alpha}} \tag{52}$$

[13] Actually, perfect partitioning is strictly speaking not required for the forward link theorem to hold, although this is not apparent in our proof. However, it is necessary for the reverse link theorem to hold.

[14] We use the notation $\overset{\text{m.s.}}{\to}$ to denote, specifically, convergence in the mean-square sense.

where

$$\overline{\alpha}(\omega;\, n] = \frac{\overline{\mathcal{E}}|A(\omega;\, n]|^2}{\mathcal{N}_0\mathcal{W}_0}. \tag{53}$$

Furthermore, in this case the corresponding SNR can be expressed as

$$\gamma_m = \frac{\mathcal{E}_m}{\overline{\mathcal{E}}}\left[\frac{1}{E\left[\frac{1}{1+\overline{\alpha}}\right]} - 1\right] \tag{54}$$

which may be further simplified using methods described in [1]. In fact, as we will discuss further in Section V-A, when $\mathcal{E}_m = \overline{\mathcal{E}}$, these results specialize to precisely those obtained in [1].

2) The Reverse Link: The following theorem summarizes the characteristics of the composite channel on the reverse link. We emphasize that in this scenario we are assuming completely uncoordinated (i.e., fully asynchronous) transmissions from mobiles to the base. A proof is again provided in Appendix III.

Theorem 2 (Reverse Link): Let $x_m[n]$ be mutually uncorrelated sequences of zero-mean, uncorrelated symbols, each with energy $\mathcal{E}_m$, and let $a_m[n;\, k]$ and $w[n]$ be as defined in (2) with the channel kernels being statistically independent. Furthermore, let $c_{mi}[n;\, k]$ denote the kernel of the linear system formed by cascading the channel seen by user m whose kernal is $a_m[n;\, k]$, with the equalizer corresponding to the detection of user i, whose kernel is $b_i[n;\, k]$, i.e.,

$$c_{mi}[n,\, k] = \sum_l b_i[n;\, l]a_m[n-l;\, k-l]. \tag{55}$$

Finally, suppose the $c_{mi}[n;\, k]$ and $b_m[n;\, k]$ are admissibly ergodic kernels in the sense of Definition 1, and let $\hat{x}_m[n]$ be defined via (41) and (40). Then, as $\mathcal{D}_h \to \infty$ (infinite dispersion) and $\chi_h \to \infty$ (perfect partitioning), we have, for each n

$$\hat{x}_m[n] \overset{\text{m.s.}}{\to} E[C_{mm}]x_m[n] + v_m[n] \tag{56}$$

where the $v_m[n]$ are mutually uncorrelated, zero-mean, complex-valued, marginally Gaussian white-noise sequences that are uncorrelated with the input symbol sequences $x_m[n]$. Furthermore, the variance of the noise samples $v_m[n]$ is independent of n and satisfies

$$\operatorname{var} v_m[n] = \mathcal{N}_0\mathcal{W}_0E[|B_m|^2] + \frac{1}{M}\sum_{k=1}^{M}\mathcal{E}_k \operatorname{var}[C_{km}]. \tag{57}$$

Again, in both (56) and (57) we have omitted specification of the time sample n and frequency ω corresponding to B_m and C_{km} due to stationarity.

Again, although we defer further more general remarks until Section IV-B3, we emphasize that, as in the forward-link case, Theorem 2 implies that the composite reverse-link channels are asymptotically mutually uncorrelated, nonfading quasi-Gaussian channels with no intersymbol interference.

From Theorem 2, we observe that the SNR of the composite channel seen by the mth user is

$$\gamma_m = \frac{\mathcal{E}_m|E[C_{mm}]|^2}{\mathcal{N}_0\mathcal{W}_0E[|B_m|^2] + \frac{1}{M}\sum_{k=1}^{M}\mathcal{E}_k \operatorname{var}[C_{km}]}. \tag{58}$$

As in the forward link, it is possible to develop equalizers yielding the best possible SNR in the composite channels for the reverse link. In particular, given sufficiently slow fading that

$$C_{kl}(\omega;\, n] \approx A_k(\omega;\, n]B_l(\omega;\, n]$$

we can re-express (58) in the form

$$\gamma_m(B_m) = \frac{\mathcal{E}_m|E[A_mB_m]|^2}{\mathcal{N}_0\mathcal{W}_0E[|B_m|^2] + \frac{1}{M}\sum_{k=1}^{M}\mathcal{E}_k \operatorname{var}(A_kB_m)}. \tag{59}$$

In turn, the following lemma directly establishes the optimum equalizer for the mth user, viz.

$$B(\omega;\, n] \propto \frac{A_m^*(\omega;\, n]}{1 + \frac{1}{M}\sum_{k=1}^{M}\alpha_k(\omega;\, n]}, \tag{60}$$

where

$$\alpha_m(\omega;\, n] = \frac{\mathcal{E}_m|A_m(\omega;\, n]|^2}{\mathcal{N}_0\mathcal{W}_0} \tag{61}$$

is the SNR at the receiver corresponding to the mth user. A proof of the lemma is provided in Appendix IV.

Lemma 1: Let $A_1, A_2, \cdots, A_M$ denote a collection of statistically independent, complex-valued, zero-mean Gaussian random variables, each with finite variance, and let $\mathcal{N}_0\mathcal{W}_0$ and $\mathcal{E}_1, \mathcal{E}_2, \cdots, \mathcal{E}_M$ be arbitrary real, nonnegative weights. Then the function $\gamma_m(B_m)$ defined in (59) satisfies

$$\frac{\gamma_m(B_m)}{M} \le \left(E\left[\frac{1 + \frac{1}{M}\sum_{k\neq m}\alpha_k}{1 + \frac{1}{M}\sum_k \alpha_k}\right]\right)^{-1} - 1 \tag{62}$$

where the α_k are as defined in (61). Furthermore, equality in (62) holds when

$$B \propto \frac{A_m^*}{1 + \frac{1}{M}\sum_{k=1}^{M}\alpha_k}.$$

3) General Remarks: Several aspects of both the interpretation and the implications of Theorems 1 and 2 are worth developing in more detail.

First, it is important to emphasize that these theorems do not establish that the composite channels are truly Gaussian channels. For example, although we argue that the additive noise sequence in the composite channel models is marginally Gaussian, we do not assert that these noise samples are actually jointly Gaussian. More generally, while these theorems describe the second-order properties of the composite channels, it should be stressed that they say very little about higher order statistical dependencies.[15] Indeed, while they establish that the collection of noises and coded streams are mutually uncorrelated, there is no claim of full mutual independence. Nevertheless, as we will see in Section V, useful approximations are obtained by modeling the composite channel as truly Gaussian and thereby ignoring these residual statistical dependencies.

[15] In fact, because of the emphasis on second-order properties, versions of these theorems hold even when the original channel noises and kernels are not Gaussian.

It is also useful to note that the additive noise in the composite channel model can be viewed as consisting of three components. Indeed, from both (48) and (57) we see that one component is due to the receiver noise in the original fading channel, while another is due to co-channel interference from other users. However, the third component is a form of self-interference generated as a by-product of the modulation, and thus the total noise power has a term that depends on the transmitted signal power. Collectively, these factors, in turn, give rise to the rather special equalizer structure which is optimum for such systems. In particular, we note that the optimum equalizers for these systems are minimum mean-square-error-type equalizers in contrast to the matched-filter-type equalizers associated with traditional CDMA systems.

It should also be emphasized that in establishing Theorems 1 and 2, both the dispersion and partitioning characteristics of the signature set are important, as the proofs of these theorems reveal. In particular, it is perfect dispersion that leads to the absence of fading and intersymbol interference in the composite channels, while it is perfect partitioning that leads to mutually uncorrelated, identical white-noise characteristics in the composite channels.

In addition, while Theorems 1 and 2 establish asymptotic results which involve signature sequences having infinite temporal spread ($N \rightarrow \infty$), it is important to note that the asymptotic behavior can, in fact, be approximated arbitrarily closely with realizable, finite-spread signature sets. In fact, it this approximation property that underlies the practical importance of these theorems.

In general, the temporal spread required to achieve a given level of approximation to the results of the theorems depends on the coherence time characteristics of the fading. Specifically, analogous to the results for spread-response precoding in [1], if N' is the spread required in the case of memoryless fading, then the spread required when the coherence time (in samples) is τ_a is

$$N = N'(\tau_a + 1).$$

Thus a larger coherence time implies that greater delay must be incurred to achieve a given level of performance. This, of course, is true of communication over fading channels in general. However, it is important to recognize that the delay constraints in spread-signature CDMA are no worse than in other systems employing, for example, interleaving.

Although greater coherence times require longer signature sequences, it is important to note that the computational requirements need not grow with coherence time. In fact, the required number of *nonzero* coefficients in each signature sequence is independent of the coherence time. In particular, to match the coherent time characteristics of a channel of interest, it suffices to upsample some prototype set of signature sequences (such as those developed in Section III-A) to achieve the necessary temporal spread. Furthermore, we note that the energy, dispersion, partitioning, and computational characteristics are all unaffected by such upsampling.

While this upsampling approach to coherence time matching is also used with spread-response precoding as described in [1], an important difference in the case of spread-signature CDMA is that the upsampling factor K cannot be freely chosen. In particular, in order to preserve orthogonality among the signatures, we may only upsample the signatures by an integer K that is not a multiple of a prime factor of the number of users M.[16] Hence, if the $h_m[n]$ are a set of prototype maximally spread signature sequences applicable to memoryless fading, the signature sequences applicable when the coherence time is τ_a are given by

$$h_m^{(\tau_a)}[n] = \begin{cases} h_m[n/K_0], & n = \cdots, -K_0, 0, K_0, 2K_0, \cdots \\ 0, & \text{otherwise} \end{cases} \tag{63}$$

where K_0 denotes the smallest integer that is not less than $\tau_a + 1$ and is not a multiple of a prime factor of M.

V. Performance

In this section we explore both the effective capacity and bit-error rate characteristics of spread-signature CDMA systems. Again, we examine the forward and reverse links separately so as to emphasize some important differences between these cases.

A. The Forward Link

Due to the coordinated nature of the transmission, performance on the forward link generally follows immediately from the results presented for single-user systems in [1]. Indeed, on the forward link, it is typical to choose

$$\mathcal{E}_1 = \mathcal{E}_2 = \cdots = \mathcal{E}_M = \overline{\mathcal{E}} \triangleq \mathcal{E}$$

in which case the optimum equalizer (52) and the optimum SNR (54) both specialize to precisely those derived in the single-user scenario developed in [1]. Furthermore, since forward link performance for any m coincides with reverse link performance for $M = 1$, we will ultimately rederive these results as special cases in Section V-B.

While many of the performance characteristics on the forward link may be directly extracted from [1], those concerning performance with realizable (finite-spread) signature sets cannot. Accordingly, we depict forward link performance obtained with realizable signature sets in Fig. 4. Specifically, we plot realizable uncoded quadrature phase-shift keying (QPSK) bit-error rate performance in Rayleigh fading as a function of SNR per bit as measured through Monte Carlo simulations. In these simulations we use the maximally spread signature sets of dimension $M = 2$ developed in Section III-A, and the dash-dotted and dashed curves indicate the performance corresponding to $N' = 32$ and $N' = 128$, respectively. For comparison, the solid curve corresponds to the asymptotic performance obtained with infinite temporal spread ($N' \rightarrow \infty$).

More generally, the single-user scenario ($M = 1$) warrants further discussion. As remarked earlier, no nontrivial finite-spread orthogonal signatures for $M = 1$ exist. As a result, in [1] the orthogonality (losslessness) constraint had to be

[16] This implies, for instance, that when the number of users M is a power of two, i.e., $M = 2^J$, we can use any odd K. Likewise, for $M = 3^J$, we can use any K which is not a multiple of 3, and for $M = 6^J$, we can use any K which is not a multiple of 2 or 3, i.e., $K = 5, 7, 11, \cdots$, etc.

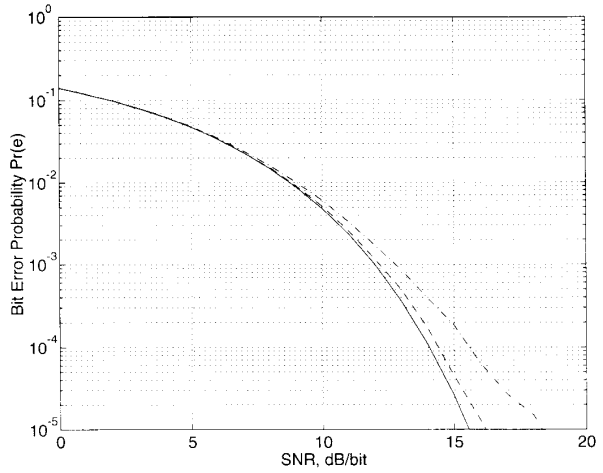

Fig. 4. Bit-error probabilities using uncoded QPSK in Rayleigh fading on the forward link. The dash-dotted and dashed curves represent the performance obtained using maximally spread signature sets with $N' = 32$ and $N' = 128$, respectively. The solid line represents the ideal performance bound ($N' \to \infty$).

relaxed in developing realizable precoders. In turn, this led to a corresponding degradation in the precoder performance. However, from within the broader framework of this paper, we can see that orthogonal signature sets corresponding to $M \geq 2$ can also be usefully applied to single-user precoding problems. In particular, we may distribute successive symbols in a stream $x[n]$ among M different substreams $x_m[n]$ by periodic subsampling, i.e.

$$x_m[n] = x[nM + m - 1]$$

and then use an orthogonal spread signature set of order M to implement perfectly lossless precoding. At the receiver, the substreams may be demodulated from the signature sequences, and appropriately reintegrated into the single stream $\hat{x}[n]$.

This strategy for implementing lossless precoding has a conceptually rather useful interpretation. Specifically, the cyclic distribution of symbols among substreams may, itself, be interpreted as a lossless system, and, hence, in effect what we construct in this manner is a linear periodically time-varying precoder.[17] Hence, we see that by adopting this more general precoder structure we are able to achieve lossless spread-response precoding with finite-length filters.

In light of these observations, we see that the curves in Fig. 4 also correspond to the single-user performance that is achievable using the improved precoders. And, comparing Fig. 4 to [1, Fig. 5], we see that significantly better performance is achieved for a given length constraint (N') when we have perfect orthogonality (losslessness).

B. The Reverse Link

The performance characteristics on the reverse link are dramatically different than those on the forward link due the uncoordinated nature of the transmissions, as we now illustrate. We begin by noting that, in practice, on the reverse link power control is generally employed to adjust the transmitter power for each user so that the average received power from each user is the same, i.e., for all users m, the SNR in the corresponding original channel is

$$E[\alpha_m(\omega; n)] \triangleq 1/\zeta_0 \tag{64}$$

where $\alpha_m(\omega; n]$ is as defined in (61). Indeed, such power control is a practical technique for mitigating the vulnerability of CDMA systems to, among other problems, near-far effects [2].

Some important insights into the potential capacity of spread-signature CDMA systems arise out of the theorems of Section IV-B. Theorem 2, in particular, suggests that the composite quasi-Gaussian channel seen by the mth user has a "capacity" given by

$$\mathcal{C}_m = \mathcal{W}_0 \log(1 + \gamma_m) \tag{65}$$

where γ_m is the SNR in the composite channel of the mth user. However, we emphasize that caution must be exercised in interpreting this notion of capacity. In particular, we note that this measure of capacity ignores all statistical effects of greater than second order in the composite channels—despite the fact that such effects can in principle be exploited to yield still higher throughputs. Nevertheless, the particular concept of constrained capacity defined here has a useful interpretation as we will develop. In particular, it provides a measure of throughput that can be achieved when traditional forms of coding are superimposed on our CDMA system.

Convenient expressions can be obtained for the composite channel SNR which maximizes this effective capacity. In particular, from Lemma 1, we have that when we use optimum equalization, γ_m can be expressed as

$$\frac{\gamma_m}{M} = \frac{1}{\beta_m} - 1 \tag{66}$$

where

$$\beta_m = E\left[\frac{1 + \frac{1}{M}\sum_{k \neq m} \alpha_k}{1 + \frac{1}{M}\sum_k \alpha_k}\right]. \tag{67}$$

Under our power control assumption, β_m as defined in (67) as independent of m, and thus we simply use β_0, γ_0, and $\mathcal{C}$ to denote the quantities (66), (67), and (65), respectively. Furthermore, in this case, by exploiting symmetry (67) can be expressed in closed form in terms of the exponential integral. In particular, we have the following Lemma, whose proof is provided in Appendix V.

Lemma 2: Let $v_1, v_2, \cdots, v_M$ be independent, identically distributed exponential random variables with mean $1/\mu$. Then for any $1 \leq m \leq M$

$$E\left[\frac{1 + \sum_{k \neq m} v_k}{1 + \sum_k v_k}\right] = \frac{M-1}{M} + \frac{\mu^M}{M!} \cdot \left[(-1)^{M+1} e^{\mu} E_1(\mu) + \sum_{k=0}^{M-2} (-1)^{M-k} \frac{k!}{\mu^{k+1}}\right] \tag{68}$$

[17] We remark as an aside that traditional interleavers are essentially trivial examples of such linear periodically time-varying systems.

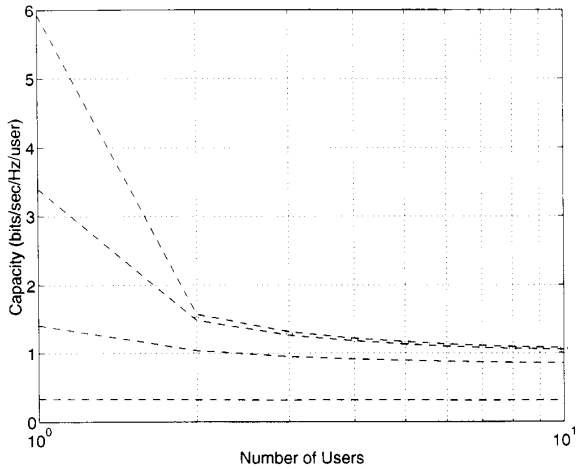

Fig. 5. Reverse-link capacity per user as a function of the number of users M. The successively higher curves correspond to SNR's of -5, 5, 15, and 25 dB. Note that the capacities corresponding to $M = 1$ also coincide with forward-link performance with any number of users. The connecting dashed lines have no special interpretation; they are provided as visual aides only.

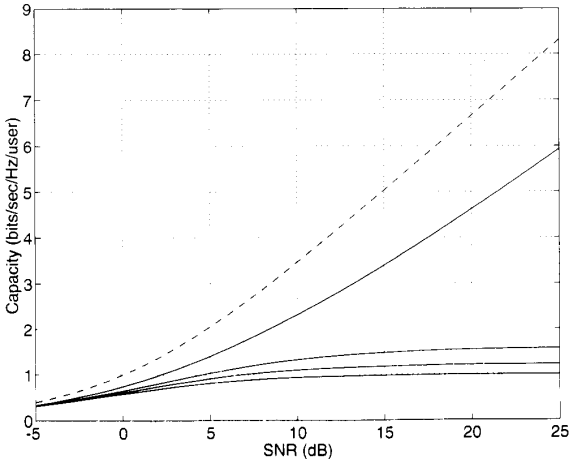

Fig. 6. Capacity per user as a function of SNR. The successively lower solid curves correspond to reverse-link transmission with $M = 1$, $M = 2$, $M = 4$, and $M \to \infty$ users. Note that the curve for $M = 1$ also coincides with forward-link capacity with any number of users. The dashed line indicates the capacity of the corresponding Gaussian channel.

where

$$E_1(\nu) = \int_{\nu}^{\infty} \frac{e^{-t}}{t}\, dt \tag{69}$$

is the exponential integral [19].

Thus using Lemma 2 with $v_k = \alpha_k/M$ we immediately obtain that (67) can be expressed as

$$\beta_0 = \frac{M-1}{M} + \frac{(M\zeta_0)^M}{M!} \cdot \left[(-1)^{M+1} e^{M\zeta_0} E_1(M\zeta_0) + \sum_{k=0}^{M-2} (-1)^{M-k} \frac{k!}{(M\zeta_0)^{k+1}} \right]. \tag{70}$$

Hence, evaluating (65) via (66) and (70), we obtain relationships for the capacity per user as a function of the number of users M, the SNR, and the bandwidth per user. In Fig. 5 we plot capacity per user as a function of M at various levels of SNR, while in Fig. 6 we plot capacity per user as a function of SNR for various values of M, with the Gaussian channel capacity included for comparison.

Note from Fig. 6 that for $M \geq 2$ the reverse link capacity appears to saturate at high SNR, with the saturation level depending on the number of users. This is, in fact, the case, and it reflects the fact that reverse-link performance is fundamentally interference-limited rather than noise-limited. This phenomenon, which is a direct consequence of the constrained receiver structure we employ, is well known. see, e.g., Verdú [20]. While it is possible to design multiple-access systems that are strictly noise-limited, this requires the use of receivers employing joint detection strategies. Unfortunately, joint detection is, in general, computationally very intensive, particularly when the number of users in the system is large [21]. For these reasons, such receivers are often considered impractical.

To verify the interference-limited behavior, let us consider the high-SNR regime performance in more detail. In this case, we may use the series expansion [19]

$$E_1(\nu) = -\Gamma_0 - \ln \nu - \sum_{k=1}^{\infty} \frac{(-1)^k \nu^k}{k k!} \tag{71}$$

with $\Gamma_0 = 0.57721\cdots$ denoting Euler's constant, to show that at high SNR ($\zeta_0 \to 0$), (70) satisfies

$$\beta_0 \to \frac{M-1}{M}. \tag{72}$$

Thus the asymptotic capacity on the reverse link in this regime is

$$\mathcal{C} \sim \log\left(\frac{2M-1}{M-1}\right). \tag{73}$$

Hence, (73) implies that the resulting capacity is finite, consistent with the saturation behavior apparent in Fig. 6.

Another important asymptotic regime to explore is the large number of user scenarios. Fortunately, as $M \to \infty$, convenient closed-form expression are possible. In particular, since the α_k are independent, identically distributed random variables, we have, by the law of large numbers

$$\frac{1}{M}\sum_{k=1}^{M} \alpha_k \to 1/\zeta_0, \qquad \text{as } M \to \infty.$$

Hence, we get

$$\gamma_0 \to \frac{1}{1+\zeta_0} \tag{74}$$

and, in turn, (65) becomes

$$\mathcal{C} \to \mathcal{W}_0 \log\left(\frac{2+\zeta_0}{1+\zeta_0}\right). \tag{75}$$

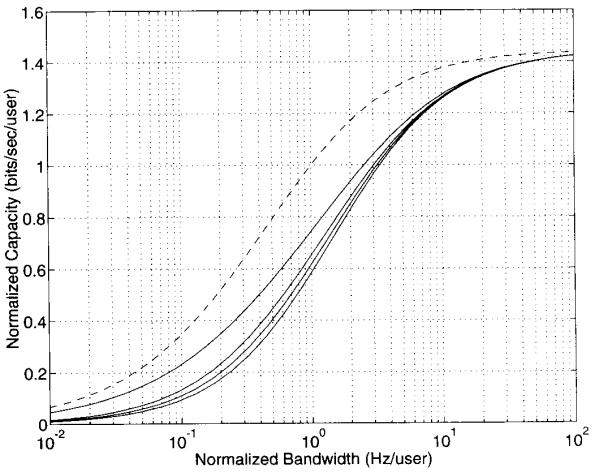

Fig. 7. Capacity per user as a function of bandwidth. The successively lower solid curves correspond to reverse-link transmission with $M = 1$, $M = 2$, $M = 4$, and $M \to \infty$ users, respectively. Note that the $M = 1$ curve for the reverse link coincides with the performance of the forward link with any number of users. The dashed line corresponds to the capacity of the Gaussian channel.

Note from (75) that when the system contains large numbers of users, we have, regardless of the transmitter power used, $\mathcal{C}/\mathcal{W}_0 < 1$ bit/s/Hz with $\mathcal{C}/\mathcal{W}_o \to 1$ bit/s/Hz as $\zeta_0 \to 0$.

It is also significant that in this case, the equalizer structure simplifies substantially as well. Again, via the law of large numbers we get

$$B \propto A_m^* \tag{76}$$

the familiar matched filter equalizer, which we note is substantially easier to implement than the optimum equalizer for finite M. Fortunately, the asymptotic performance is achieved for fairly moderate values of M as Fig. 5 reveals, so that in practice this simpler equalizer can frequently be used.

Let us now turn our attention to the SNR-limited setting, and consider the large-bandwidth behavior. In Fig. 7 we plot normalized capacity as a function of bandwidth per user for various values of M, with the Gaussian channel capacity included for comparison. Several general remarks regarding Fig. 7 are appropriate. First, as in the case of the Gaussian channel, the capacity in our multiuser fading environment increases monotonically with bandwidth per user. Second, the horizontal distance between the $M = 1$ and $M \geq 2$ curves quantifies how much additional bandwidth is required to compensate for the absence of coordination on the reverse link.

Perhaps the most important observation from Fig. 7, however, is that the infinite bandwidth capacity is identical to that of the Gaussian channel. To verify this property, we note that using the asymptotic series expansion [19]

$$E_1(\nu) = e^{-\nu}\sum_{k=0}^{\infty}(-1)^k\frac{k!}{\nu^{k+1}}, \qquad \text{large } \nu \tag{77}$$

we have that for large $\mathcal{W}_0$ (i.e., large ζ_0)

$$\beta_0 \sim 1 + \sum_{k=0}^{\infty}\frac{(k+M)!}{M!}\frac{(-1)^{k+1}}{(M\zeta_0)^{k+1}}. \tag{78}$$

Using (78) in (66), we see that for large $\mathcal{W}_0$

$$\gamma_0 \sim \frac{M}{M\zeta_0 - 1} \tag{79}$$

However, since γ_0 in (79) is small, (65) can be expressed asymptotically as

$$\mathcal{C} \sim \mathcal{W}_0\gamma_0 = \frac{M\mathcal{W}_0}{M\zeta_0 - 1}. \tag{80}$$

Using the fact that (61) and (64) imply

$$\mathcal{W}_0/\zeta_0 = \frac{\mathcal{E}_m E[|A_m|^2]}{\mathcal{N}_0}$$

we verify from (80) that

$$\mathcal{C} \to \frac{\mathcal{E}_m E[|A_m|^2]}{\mathcal{N}_0} \tag{81}$$

which we emphasize is independent of m by our power control assumption. Finally, we note that (81) is, of course, the capacity of the infinite-bandwidth Gaussian channel.

C. Exploiting Additional Processing Gain

For reverse-link communication, co-channel interference is such that even at high SNR, the SNR γ_0 of the composite quasi-Gaussian channel for each user is low. In particular, using (72) in (66) we see that regardless of the available bandwidth or power we have

$$0 < \gamma_0 < \frac{M}{M-1}$$

for $M \geq 2$. This means that in order to achieve a throughput per user anywhere near that predicted by the capacity calculations in Section V-B, an enormous amount of coding is required. Conversely, without the use of coding, bit-error-rate performance on the reverse link will be invariably poor.

As an alternative to coding, one can consider exploiting simple spread-spectrum processing gain to raise γ_0 to a level sufficient for acceptable bit-error-rate performance. Although, as we shall see, direct coding is always preferable in terms of efficiency, using simple processing gain is appealing in terms of its substantial ease of implementation and reduced computational complexity.

Augmenting our M-user system model to incorporate such processing gain is straightforward. In essence, we expand the bandwidth per user while fixing the symbol rate by replacing the up- and downsampling rates in Figs. 1 and 3 with an integer L satisfying $L > M$. The resulting bandwidth expansion factor or processing gain is then

$$\rho = L/M. \tag{82}$$

With this change, the SNR γ_m of the composite channel becomes

$$\frac{\gamma_m}{L} = \frac{1}{\beta_m} - 1 \tag{82'}$$

where

$$\beta_m = E\left[\frac{1+\frac{1}{L}\sum_{\substack{k=1\\k\neq m}}^{M}\alpha_k}{1+\frac{1}{L}\sum_{k=1}^{M}\alpha_k}\right] \tag{83}$$

and with α_k as in (61). Again, assuming power control and using Lemma 2 with $v_k = \alpha_k/L$ we can express (83) in closed form as

$$\beta_0 = \frac{M-1}{M} + \frac{(L\zeta_0)^M}{M!} \cdot \left[(-1)^{M+1}e^{L\zeta_0}E_1(L\zeta_0) + \sum_{k=0}^{M-2}(-1)^{M-k}\frac{k!}{(L\zeta_0)^{k+1}}\right]. \tag{84}$$

In the remainder of this section, we focus on the large number of users ($M \to \infty$) scenario. In this case, again using the law of large numbers, we get

$$\gamma_0 \sim \frac{1}{\zeta_0 + 1/\rho} \tag{85}$$

where ρ is as given by (82). At high SNR (i.e., when the receiver noise is negligible), (85) further simplifies to

$$\gamma_0 \sim \rho.$$

The use of processing gain permits a tradeoff between bit-error rate and bandwidth. In particular, from (85) we see that larger processing gains invariably give rise to improved bit-error-rate performance. However, this improvement is obtained at the expense of bandwidth. From an information-theoretic point of view, this particular tradeoff is not efficient. To see this, note that if we apply coding on top of this new system that exploits processing gain, the apparent capacity per user per unit bandwidth is

$$\frac{\mathcal{C}}{\mathcal{W}_0\rho} = \frac{1}{\rho}\log(1+\gamma_0) = \frac{1}{\rho}\log\left(1+\frac{1}{\zeta_0+1/\rho}\right) \tag{86}$$

where the last equality follows from (85). In Fig. 8, we use (86) to plot capacity per user per unit bandwidth as a function of the processing gain ρ in the large number of users limit $M \to \infty$. We note that the effective capacity achievable with additional coding falls monotonically with ρ, and that the case $\rho = 1$ corresponds to our original system, i.e., the system without processing gain. This is because the bandwidth expansion incurred by using a larger processing gain ρ more than offsets the increase in the SNR per symbol achieved. In fact, it is straightforward to show from (86) that $\mathcal{C} \to 0$ as $\rho \to \infty$.

Despite the inherent bandwidth inefficiency, exploiting processing gain is a highly practical technique and enjoys widespread use. Let us consider, for example, the bit-error-rate performance of uncoded QPSK (quadrature phase-shift keying) using spread-signature CDMA with M users and processing gain $\rho = L/M$, some integer L. In this case, again assuming the use of power control, the bit-error probability is given by

$$\mathcal{P} = \mathcal{Q}(\sqrt{\gamma_0}) \tag{87}$$

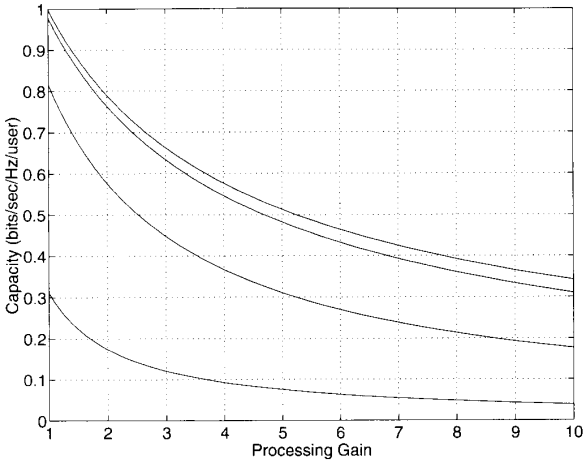

Fig. 8. Capacity per user per unit bandwidth as a function of processing gain ρ, where the number of users satisfies $M \to \infty$. The successively higher curves correspond to SNR's of -5, 5, 15, and 25 dB.

where

$$\mathcal{Q}(\nu) = \frac{1}{\sqrt{2\pi}}\int_{\nu}^{\infty} e^{-t^2/2}\,dt$$

and where γ_0 is given by (82′) with (84), or, in the case of large numbers of users, (85).

In Fig. 9 we plot bit-error probability as a function SNR per bit for several processing gains in the large number of user scenarios, and include comparison to conventional CDMA. In both the spread-signature and conventional CDMA systems, no channel coding is used. From this plot, it is apparent that there is an enormous advantage in using spread-signature CDMA over conventional CDMA in such uncoded systems. This is due to the fact that spread-signature CDMA is much more effective than conventional CDMA at mitigating the effects of fading even without additional coding. In particular, at high SNR and for large numbers of users, the bit-error probability of spread-signature CDMA saturates at

$$\mathcal{P} \sim \mathcal{Q}(\sqrt{\rho}) \tag{88}$$

while for conventional CDMA the bit error probability saturates at

$$\mathcal{P}_0 \sim \frac{1}{2}\left(1-\frac{1}{\sqrt{2/\rho+1}}\right). \tag{89}$$

Finally, in Fig. 10, we plot bit-error probability as a function of processing gain for several SNR values, again in the large number of users scenarios. For comparison, we also plot the performance of conventional CDMA, using (89).

VI. Concluding Remarks

Spread-signature CDMA as developed in this paper constitutes a potentially attractive alternative to conventional CDMA

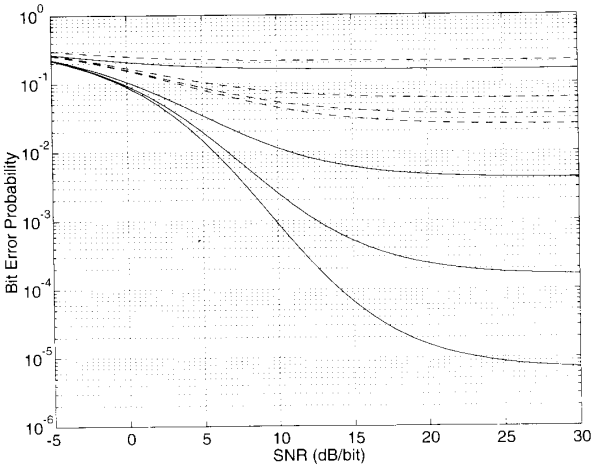

Fig. 9. Bit-error probability as a function of SNR per bit for uncoded QPSK on reverse link with $M \to \infty$ users. The successively lower solid curves correspond to the performance of spread-signature CDMA with processing gains of $\rho = 1, 7, 13, 19$. For comparison, the successively lower dashed curves correspond to the performance of conventional CDMA with the same series of processing gains. For these comparisons, no coding is used in either system.

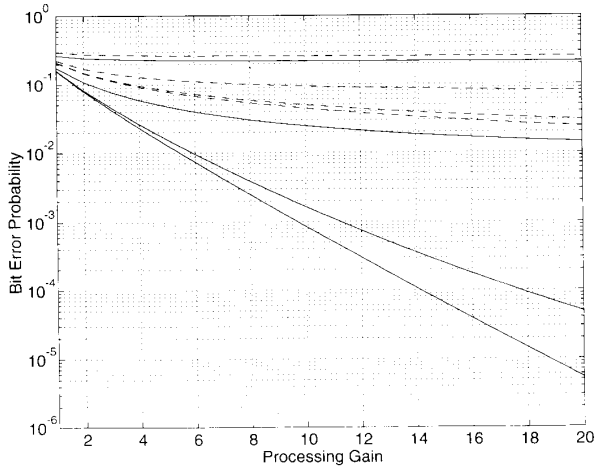

Fig. 10. Bit-error probability as a function of processing gain for uncoded QPSK on reverse link with $M \to \infty$ users. The successively lower solid curves correspond to the performance of spread-signature CDMA with SNR's of -5, 5, 15, and 25 dB/bit. For comparison, the successively lower dashed curves correspond to the performance of conventional CDMA with the same series of SNR's. For these comparisons, no coding is used in either system.

for general multiuser communication in fading environments. Indeed, the performance results suggest that by effectively combining modulation and precoding, such systems appear to offer significantly better performance.

Nevertheless, numerous issues remain to be explored. In traditional CDMA systems, coding is used to combat the effects of fading, co-channel interference, and receiver noise. However, in spread-signature CDMA systems, the effects of fading are mitigated by the precoding implicit in the modulation, leaving coding to handle only the remaining interference and noise effects. This would appear to be a favorable computational tradeoff, since in general demodulation is computationally much cheaper than decoding. However, further simulations are required to verify these computational advantages. In addition, while we have restricted our attention to single-user detector receivers, the possibility of developing viable joint detector receivers is also worth pursuing.

Other issues, both technical and practical, also warrant further investigation. Among the technical issues, an obvious question that arises concerns the extent to which the capacity expressions developed in this paper can be interpreted in a strict Shannon sense. Some of the more important practical issues which remain to be explored include receiver synchronization and peak-to-average transmitter power requirements, and equalizer sensitivity characteristics. Another practical issue concerns how these strategies behave on more realistic (and thus more complicated) fading and related channel models. From this perspective, the analysis for the highly tractable Rayleigh fading channel presented here is a good starting point for further investigation.

Among the signature design issues that warrant further investigation include developing design techniques that provide some control over the correlation structure in the signatures when subject to shifts of less than the intersymbol period M. While we impose strict orthogonality on shifts by multiples of M, we do not optimize our behavior for other shifts. The signature sets developed in Section III-A have reasonable intrasymbol shift correlations, but this would appear to be somewhat coincidental. The Welch-bound generalizations in Section III indicate some constraints, but not all. In addition, it would appear that to provide control over intrasymbol shift correlations one might have to give up the binary constraint on signature sequences, the consequences of which remain to be explored. More generally, there are several significant issues to be explored here, including how such factors affect practical system performance.

Several extensions and variations on the spread-signature scheme can also be developed within the framework of this paper. As an example, in many CDMA systems with traditional (nonlapped) signature sequences (such as the Qualcomm system), the signature sequence spans multiple symbols. This can be viewed as a system in which instead of using the same signature sequence for every symbol in a particular user's stream, each symbol is modulated onto one of several distinct signatures. Spread-signature systems can also be extended to accommodate this flexibility if desired. In fact, the approach is to generalize the single-user periodically time-varying strategy discussed in Section V-A. As a simple example for the purposes of illustration, to obtain a two-user system in which each user alternates between two signature sequences for consecutive symbols, a total of four orthogonal signatures are required and can be generated via the construction of Section III-A. A particular user's stream is then constructed by creating two parallel symbol substreams via subsampling, each of which is modulated on one of that user's two signature sequences and then the resulting modulated substreams are superimposed.

APPENDIX I
LINEAR RANDOMLY TIME-VARYING SYSTEMS

We adopt the following notation for linear randomly time-varying systems corresponding to wide-sense-stationary uncorrelated scattering. We begin by using $f[n;\, k]$ to denote the kernel of a discrete-time linear system, corresponding to the response of the system at time n to a unit sample at time $n-k$. Hence, the response of the system to an input $x[n]$ is

$$y[n] = \sum_k f[n;\, k]x[n-k].$$

The time-variant system frequency response associated with this system is denoted by

$$F(\omega;\, n] = \sum_k f[n;\, k]e^{-j\omega k} \tag{90}$$

and represents the response of the system to complex exponential $e^{j\omega n}$. For stationary systems, we define the system correlation function by

$$R[m;\, k] = E[\tilde{f}[n;k]\tilde{f}^*[n-m;k]]$$

where

$$\tilde{f}[n{:}\, k] = f[n;\, k] - E[f[n;\, k]]$$

and the system scattering function by

$$S(\lambda;\, k] = \sum_m R[m;\, k]e^{-j\lambda m}.$$

When the system is characterized by uncorrelated scattering we have both

$$E[f[n;\, k]] = E[f[n;\, 0]]\delta[k]$$

and

$$E[\tilde{f}[n;\, k]\tilde{f}^*[n-m;\, l]] = R[m;\, k]\delta[k-l].$$

This makes $F(\omega;\, n]$ defined in (90) wide-sense-stationary in both ω and n, a property we exploit extensively.

Another useful characterization of such systems is in terms of the associated spaced-frequency spaced-time correlation function, which is given by

$$\begin{aligned}\Psi(\omega;\, m] &= \sum_k R[m;\, k]e^{-j\omega k} \\ &= E[\tilde{F}(\theta;\, n]\tilde{F}^*(\theta-\omega;\, n-m]]\end{aligned}$$

where

$$\tilde{F}(\omega;\, n] = F(\omega;\, n] - E[F(\omega;\, n]].$$

In turn, we define the system Doppler power spectrum by

$$\Upsilon(\lambda) = \sum_m \Psi(0;\, m]e^{j\lambda m}.$$

Finally, the multipath intensity profile or delay power spectrum of the system is

$$\Pi[k] = R[0,\, k] = \operatorname{var} f[n;\, k]$$

so the total power is

$$\operatorname{var} F(\omega;\, n] = \Psi(0;\, 0] = \sum_k \Pi[k].$$

APPENDIX II
MAXIMALLY SPREAD SIGNATURE SEQUENCES

Coefficients are first converted to a binary sequence, with $1/\sqrt{N}$ represented by "1" and $-1/\sqrt{N}$ represented by "0," then replaced with the hexidecimal equivalent.

M	N	$\mathbf{h}[n]$
2	4	E
		D
4	4	F
		A
		C
		9
2	8	ED
		E2
8	8	FF
		AA
		CC
		99
		F0
		A5
		C3
		96
2	16	EDE2
		ED1D
4	16	FAC9
		F5C6
		FA36
		F539
2	32	EDE2ED1D
		EDE212E2
2	64	EDE2ED1DEDE212E2
		EDE2ED1D121DED1D
4	64	FAC9F5C6FA36F539
		FAC90A39FA360AC6
		FAC9F5C605C90AC6
		FAC90A3905C9F539
8	64	FFAACC99F0A5C396
		FF55CC66F05AC369
		FFAA3366F0A53C69
		FF553399F05A3C96
		FFAACC990F5A3C69
		FF55CC660FA53C96
		FFAA33660F5AC396
		FF5533990FA5C369
2	128	EDE2ED1DEDE212E2EDE2ED1D121DED1D
		EDE2ED1DEDE212E2121D12E2EDE212E2
2	256	EDE2ED1DEDE212E2EDE2ED1D121DED1DEDE2ED1DEDE212E2121D12E2EDE212E2
		EDE2ED1DEDE212E2EDE2ED1D121DED1D121D12E2121DED1DEDE2ED1D121DED1D
4	256	FAC9F5C6FA36F539FAC90A39FA360AC6FAC9F5C605C90AC6FAC90A3905C9F539
		FAC9F5C6FA36F5390536F5C605C9F539FAC9F5C605C90AC60536F5C6FA360AC6
		FAC9F5C6FA36F539FAC90A39FA360AC605360A39FA36F5390536F5C6FA360AC6
		FAC9F5C6FA36F5390536F5C605C9F53905360A39FA36F539FAC90A3905C9F539

APPENDIX III
PROOFS OF THEOREMS 1 AND 2

It is convenient to develop some intermediate results for a family of related systems. Let $\mathcal{S}_{ij}\{\cdot\}$ denote a linear system which is the cascade of a rate-M upsampler, an LTI system whose unit-sample response is $h_i[n]$, a linear time-varying system whose kernel is $f_{ij}[n;\, k]$, another LTI system with unit-sample response $h_j[-n]$, and finally a rate-M downsampler. Hence

$$\begin{aligned}q[n] &= \mathcal{S}_{ij}\{p[n]\} \\ &= \sum_{m,\,l,\,k} f_{ij}[m;\, l]h_j[m-nM]h_i[m-l-kM]p[k]\end{aligned} \tag{91}$$

and it is straightforward to show that the kernel of this system is

$$u_{ij}[n;\, k] = \sum_{m,\,l} f_{ij}[nM+m;\, kM+l]h_j[m]h_i[m-l]. \tag{92}$$

We begin with the following lemma.

Lemma 3: Let $h_i[n]$ and $h_j[n]$ be chosen from an set of M orthogonal signatures, and let $f_{ij}[n;\, k]$ for $j = 1, 2, \cdots, M$ be an admissibly ergodic family of kernels in the sense of Definition 1. Then, with $\mathcal{D}_h$ and χ_h as defined in (21) and (29), respectively, as $\mathcal{D}_h \to \infty$ and $\chi_h \to \infty$, the kernel (92) obeys

$$u_{ij}[n;\, k] \overset{\text{m.s.}}{\to} E[F_{ii}]\delta[k]\delta[i-j] \triangleq u_{ij}[k] \tag{93}$$

and

$$\sum_k \tilde{u}_{ij}[n;\, n-k]\tilde{u}^*_{ij'}[m;\, m-k] \overset{\text{m.s.}}{\to} \frac{1}{M} \cdot \text{var}\,[F_{ij}]\delta[n-m]\delta[j-j'] \tag{94}$$

where

$$\tilde{u}_{ij}[n;\, k] = u_{ij}[n;\, k] - u_{ij}[k].$$

Proof: Using (45a) with (92), we obtain

$$\begin{aligned} E[u_{ij}[n;\, k]] &= E[F_{ij}]\sum_l h_j[l]h_i[l+kM] \\ &= E[F_{ii}]\delta[i-j]\delta[k] \end{aligned} \tag{95}$$

and

$$\tilde{u}_{ij}[n;\, k] = \sum_{m,\, l} \tilde{f}_{ij}[nM+m;\, kM+l]h_j[m]h_i[m-l] \tag{96}$$

where $\tilde{f}_{ij}[n;\, k]$ is as defined in (42).

From (96) we get

$$\begin{aligned} E[|\tilde{u}_{ij}[n;\, k]|^2] = \sum_{m,\, m',\, l} & R^{ij'}_{ij}[m-m';\, kM-l] \\ & \cdot h_j[m]h_j[m']h_i[l+m]h_i[l+m'] \end{aligned} \tag{97}$$

where $R^{ij}_{ij}[m;\, k]$ is as defined in (45b). Applying, in order the triangle inequality and the Cauchy inequality, (97) can be bounded by

$$E[|\tilde{u}_{ij}[n;\, k]|^2] \le \varphi(h_i)\varphi(h_j) \tag{98}$$

where

$$\varphi^2(g) = \sum_{m,\, m',\, l} |R^{ij}_{ij}[m-m';\, kM-l]|g^2[m]g^2[m']. \tag{99}$$

Applying the Cauchy inequality again to $\varphi^2(g)$, however, gives after some simplification, and using (45d)

$$\varphi^2(g) \le S_{R^{ij}_{ij}}/\mathcal{D}_g$$

where

$$\mathcal{D}_g = \left(\sum_n g^4[n]\right)^{-1}.$$

Hence

$$E[|\tilde{u}_{ij}[n;\, k]|^2] \le \frac{S_{R^{ij}_{ij}}}{\sqrt{\mathcal{D}_{h_i}\mathcal{D}_{h_j}}} \tag{100}$$

which tends to zero as $\mathcal{D}_h \to \infty$. Collectively, (95) and (100) establish (93).

To show (94), we begin by noting that

$$\begin{aligned} \rho^{ij'}_{ij}[n,\, m] &\triangleq \sum_k \tilde{u}_{ij}[n;\, n-k]\tilde{u}^*_{ij'}[m;\, m-k] \\ &= \sum_{s,\, s'}\sum_{t,\, t'} \tilde{f}_{ij}[nM+s;\, t]\tilde{f}^*_{ij'}[mM+s';\, t'] \\ &\quad \cdot h_j[s]h'_j[s'] \\ &\quad \cdot \Theta_{h_i}[nM+s-t,\, mM+s'-t'] \end{aligned}$$

where $\Theta_{h_i}[n,\, m]$ is as defined in (25).

Using (45b), we obtain

$$\begin{aligned} E[\rho^{ij'}_{ij}[n,\, m]] = \sum_{s,\, s',\, t} & R^{ij'}_{ij}[(n-m)M+s-s';\, t] \\ & \cdot h_j[s]h_{j'}[s'] \\ & \cdot \Theta_{h_i}[nM+s-t,\, mM+s'-t] \end{aligned}$$

which, with

$$\begin{aligned} \check{\rho}^{ij'}_{ij}[n,\, m] \triangleq \sum_{s,\, s',\, t} & R^{ij'}_{ij}[(n-m)M+s-s';\, t]h_j[s]h_{j'}[s'] \\ & \cdot \Theta_{h_i}[nM+s-t,\, mM+s'-t] \end{aligned} \tag{101}$$

and using (27), can be rewritten as

$$\begin{aligned} E[\rho^{ij'}_{ij}[n,\, m]] &= \check{\rho}^{ij'}_{ij}[n,\, m] \\ &\quad + \frac{1}{M}\sum_t R^{ij'}_{ij}[0;\, t]\sum_s h_j[s]h_{j'}[s+(n-m)M] \\ &= \check{\rho}^{ij'}_{ij}[n,\, m] + \frac{1}{M}\,\text{var}\,[F_{ij}]\delta[j-j']\delta[n-m]. \end{aligned} \tag{102}$$

Now applying the triangle inequality and the Cauchy inequality to (102), we obtain the bound

$$|\check{\rho}^{ij'}_{ij}[n,\, m]| \le \xi_1\xi_2 \tag{103}$$

where

$$\xi_1^2 = \sum_{s,\, s',\, t} |R^{ij'}_{ij}[(n-m)M+s-s';\, t]h_j[s]h_{j'}[s']| \tag{104}$$

and

$$\begin{aligned} \xi_2^2 = \sum_{s,\, s',\, t} & |R^{ij'}_{ij}[(n-m)M+s-s';\, t]h_j[s]h_{j'}[s']| \\ & \cdot \tilde{\Theta}^2_{h_i}[nM+s-t,\, mM+s'-t]. \end{aligned} \tag{105}$$

Applying the Cauchy inequality to (105) yields

$$\xi_2^2 \le \xi_1\xi_3 \tag{106}$$

where

$$\begin{aligned} \xi_3^2 = \sum_{s,\, s',\, t} & |R^{ij'}_{ij}[(n-m)M+s-s';\, t]h_j[s]h_{j'}[s']| \\ & \cdot \tilde{\Theta}^4_{h_i}[nM+s-t,\, mM+s'-t]. \end{aligned} \tag{107}$$

Similarly, applying the Cauchy inequality to (104) yields

$$\xi_1^4 \le \left(\sum_{s,\, s',\, t} |R_{ij}^{ij'}[(n-m)M + s - s';\, t]| h_j^2[s] \right) \cdot \left(\sum_{s,\, s',\, t} |R_{ij}^{ij'}[(n-m)M + s - s';\, t]| h_{j'}^2[s'] \right) = S_{R_{ij}^{ij'}}^2 . \tag{108}$$

Similarly, applying the Cauchy inequality to (107) yields

$$\xi_3^4 \le \left(\sum_{s,\, s',\, t} |R_{ij}^{ij'}[(n-m)M + s - s';\, t]| \cdot h_j^2[s] \tilde{\Theta}_{h_i}^4[nM + s - t,\, mM + s' - t] \right) \cdot \left(\sum_{s,\, s',\, t} |R_{ij}^{ij'}[(n-m)M + s - s';\, t]| \cdot h_{j'}^2[s'] \tilde{\Theta}_{h_i}^4[nM + s - t,\, mM + s' - t] \right) \le \frac{S_{R_{ij}^{ij'}}^2}{\chi_{h_i}^2} \tag{109}$$

where the last inequality in (109) results from using, in order, the simple bound

$$|R_{ij}^{ij'}[n;\, k]| \le S_{R_{ij}^{ij'}}^2$$

and (30).

Using (108), (109), and (106) with (110) we get

$$|\tilde{\rho}_{ij}^{ij'}[n,\, m]| \le \frac{S_{R_{ij}^{ij'}}^{5/4}}{\sqrt{\chi_{h_i}}} \tag{110}$$

which tends to zero as $\chi_h \to \infty$.

Next, we define

$$\tilde{\rho}_{ij}^{ij'}[n,\, m] = \rho_{ij}^{ij'}[n,\, m] - E[\rho_{ij}^{ij'}[n,\, m]]$$

and note

$$\tilde{\rho}_{ij}^{ij'}[n,\, m] = \sum_{s,\, s'} \sum_{k,\, k'} \tilde{d}_{ij}^{ij'}[s,\, s';\, k,\, k'] \Theta_{h_i}[s-k;\, s'-k'] \cdot h_j[s - nM] h_{j'}[s' - mM] \tag{111}$$

where $\tilde{d}_{ij}^{ij'}[s,\, s';\, t,\, t']$ is as defined in (44) and (43).

In turn, using (45c) with (111), we get

$$E[|\tilde{\rho}_{ij}^{ij'}[n,\, m]|^2] = \sum_{\substack{s,\, s' \\ k,\, k'}} \sum_{\substack{t,\, t' \\ l,\, l'}} T_{ij}^{ij'}[s - s',\, t - t',\, s - t;\, k,\, k',\, l,\, l'] \cdot \Theta_{h_i}[s-k;\, s'-k'] \Theta_{h_i}[t-l;\, t'-l'] \cdot h_j[s - nM] H_{j'}[s' - mM] h_j[t - nM] h_{j'}[t' - mM]. \tag{112}$$

Now, from a simple application of the Cauchy inequality to (25) we obtain

$$|\Theta_{h_i}[n,\, m]| \le 1. \tag{113}$$

Applying, in turn, the triangle inequality, the bound (113), and the Cauchy inequality to (112) we obtain

$$E[|\tilde{\rho}_{ij}^{ij'}[n,\, m]|^2]^2 \le \left(\sum_{\substack{s,\, s' \\ k,\, k'}} \sum_{\substack{t,\, t' \\ l,\, l'}} |T_{ij}^{ij'}[s - s',\, t - t',\, s - t;\, k,\, k',\, l,\, l']| \cdot h_j^2[s - nM] h_{j'}^2[s' - mM] \right) \cdot \left(\sum_{\substack{s,\, s' \\ k,\, k'}} \sum_{\substack{t,\, t' \\ l,\, l'}} |T_{ij}^{ij'}[s - s',\, t - t',\, s - t;\, k,\, k',\, l,\, l']| \cdot h_j^2[t - nM] h_{j'}^2[t' - mM] \right). \tag{114}$$

Applying the Cauchy inequality once again to the right-hand side terms of (114) yields

$$E[|\tilde{\rho}_{ij}^{ij'}[n,\, m]|^2]^4 \le \left(\sum_{\substack{s,\, s' \\ k,\, k'}} \sum_{\substack{t,\, t' \\ l,\, l'}} |T_{ij}^{ij'}[s - s',\, t - t',\, s - t;\, k,\, k',\, l,\, l']| \cdot h_j^4[s - nM] \right) \cdot \left(\sum_{\substack{s,\, s' \\ k,\, k'}} \sum_{\substack{t,\, t' \\ l,\, l'}} |T_{ij}^{ij'}[s - s',\, t - t',\, s - t;\, k,\, k',\, l,\, l']| \cdot h_{j'}^4[s' - mM] = \right) \cdot \left(\sum_{\substack{s,\, s' \\ k,\, k'}} \sum_{\substack{t,\, t' \\ l,\, l'}} |T_{ij}^{ij'}[s - s',\, t - t',\, s - t;\, k,\, k',\, l,\, l']| \cdot h_j^4[t - nM] \right) \cdot \left(\sum_{\substack{s,\, s' \\ k,\, k'}} \sum_{\substack{t,\, t' \\ l,\, l'}} |T_{ij}^{ij'}[s - s',\, t - t',\, s - t;\, k,\, k',\, l,\, l']| \cdot h_{j'}^4[t' - mM] \right) = \frac{S_{T_{ij}^{ij'}}^4}{\mathcal{D}_{h_j}^2 \mathcal{D}_{h_{j'}}^2} \tag{115, 116}$$

which tends to zero as $\mathcal{D}_h \to \infty$. Collectively, (102), (110), and (116) establish (94). ■

Proposition 1: Suppose that the input to the system defined by (92) is a zero-mean, white Gaussian sequence $p_i[n]$ with variance σ_i^2, and let the corresponding output sequence be $q_{ij}[n]$. Moreover, assume that for different values of i the sequences $p_i[n]$ are mutually independent. Then given the same hypotheses of Lemma 3, we have

$$q_{ij}[n] \overset{\text{m.s.}}{\to} E[F_{ii}]\delta[i-j]p_i[n] + z_{ij}[n] \tag{117}$$

where the $z_{ij}[n]$ are mutually uncorrelated, zero-mean white marginally Gaussian sequences with variances $\sigma_i^2 \operatorname{var}[F_{ij}]/M$, i.e.

$$E[z_{ij}[n]] = 0 \tag{118a}$$

$$E[z_{ij}[n]p_{i'}^*[m]] = 0 \tag{118b}$$

$$E[z_{ij}[n]z_{i'j'}[m]] = \delta[i-i']\delta[j-j']\delta[n-m] \cdot \frac{1}{M}\sigma_i^2 \operatorname{var}[F_{ij}]. \tag{118c}$$

Furthermore, we have that the sequences $q_{ij}[n]$ are zero-mean and white with variance

$$\operatorname{var} q_{ij}[n] = \delta[i-j]\sigma_i^2|E[F_{ii}]|^2 + \frac{1}{M}\sigma_i^2 \operatorname{var}[F_{ij}] \tag{119}$$

and are mutually uncorrelated for different values of j.

Proof: We begin by noting that

$$q_{ij}[n] = \sum_k u_{ij}[n;\, k]p_i[n-k]$$

can be rewritten as

$$q_{ij}[n] = E[F_{ii}]\delta[i-j]p[n] + z_{ij}[n]$$

where

$$z_{ij}[n] = \sum_k \tilde{u}_{ij}[n;\, k]p_i[n-k]. \tag{120}$$

From (120) we get immediately, since $p_i[n]$ is zero-mean, that $z_{ij}[n]$ satisfies (118a), i.e.

$$E_p[z_{ij}[n]] = 0$$

where we use $E_p[\cdot]$ to denote expectation with respect to $p[n]$ given fixed but arbitrary realizations of the kernels $f_{ij}[n;\, k]$.

In addition, from (120) we get

$$E_p[z_{ij}[n]p_{i'}^*[m]] = \sigma_i^2\delta[i-i']\tilde{u}[n;\, n-m]. \tag{121}$$

Hence, since (93) in Lemma 3 implies

$$\tilde{u}[n;\, k] \overset{\text{m.s.}}{\to} 0$$

we get, from (121), the result (118b), i.e.

$$E_p[z_{ij}[n]p_{i'}[m]] \overset{\text{m.s.}}{\to} 0.$$

Finally, using (120) we also obtain

$$\begin{aligned} &E_p[z_{ij}[n]z_{ij'}^*[m]] \\ &= \sigma_i^2\delta[i-i']\sum_{k,\,l}\tilde{u}_{ij}[n;\, k]\tilde{u}_{ij'}^*[m;\, l] \\ &\quad \cdot E_p[p_i[n-k]p_i[m-l]] \\ &= \sigma_i^2\delta[i-i']\sum_k \tilde{u}_{ij}[n;\, n-l]\tilde{u}_{ij'}^*[m;\, m-l]. \end{aligned} \tag{122}$$

Applying (94) in Lemma 3 to (122) we obtain (118c) immediately, i.e.

$$E_p[z_{ij}[n]z_{ij'}^*[m]] \to \sigma_i^2\delta[i-i']\frac{1}{M}\operatorname{var}[F_{ij}]\delta[n-m]\delta[j-j'].$$

Finally, to show that $z_{ij}[n]$ is marginally Gaussian requires a Central Limit Theorem argument. ■

A. The Forward-Link Theorem

Using Proposition 1, we can readily establish Theorem 1. In particular, due to linearity we can partition $\hat{x}_m[n]$ into two components: $\hat{x}_m^{(1)}[n]$, which is generated by the set of transmitted sequences $x_i[n]$, and $\hat{x}_m^{(2)}[n]$, which is generated by the background noise $w[n]$.

We first note that if in Proposition 1 we let $p_i[n] = x_i[n]$ and $f_{ij}[n;\, k] = c[n;\, k]$, then we readily obtain, using superposition, that

$$\hat{x}_m^{(1)}[n] = \sum_{i=1}^M q_{im}[n] \overset{\text{m.s.}}{\to} E[C]x_m[n] + v_m^{(1)}[n] \tag{123}$$

where

$$v_m^{(1)}[n] = \sum_{i=1}^M z_{im}[n].$$

Note, in addition, that due to the properties of the $z_{ij}[n]$ in Proposition 1 the $v_m^{(1)}[n]$ are mutually uncorrelated, zero-mean, white marginally Gaussian noise sequences with variances

$$\operatorname{var} v_m^{(1)}[n] = \operatorname{var}[C]\frac{1}{M}\sum_{i=1}^M \mathcal{E}_i. \tag{124}$$

Next we note that if in Proposition 1 we let

$$p_i[n] = \sum_k w[k]h_m[k-nM] \quad \text{and} \quad f_{ij}[n;\, k] = b[n;\, k]$$

then we again readily obtain that

$$\hat{x}_m^{(2)}[n] = \sum_{i=1}^M q_{im}[n] \overset{\text{m.s.}}{\to} v_m^{(2)}[n] \tag{125}$$

where the $v_m^{(2)}[n]$ are mutually uncorrelated, zero-mean, white marginally Gaussian noise sequences with variances

$$\begin{aligned} \operatorname{var} v_m^{(2)}[n] &= \mathcal{N}_0\mathcal{W}_0|E[B]|^2 + \mathcal{N}_0\mathcal{W}_0 \operatorname{var}[B] \\ &= \mathcal{N}_0\mathcal{W}_0 E[|B|^2]. \end{aligned} \tag{126}$$

Hence, combining (123) and (125) we obtain (47) where

$$v_m[n] = v_m^{(1)}[n] + v_m^{(2)}[n].$$

Furthermore, since the $x_m[n]$ and $w[n]$ are uncorrelated, we obtain (48) using

$$\operatorname{var} v_m[n] = \operatorname{var} v_m^{(1)}[n] + \operatorname{var} v_m^{(2)}[n]$$

with (124) and (126).

B. The Reverse-Link Theorem

Using Proposition 1, we can also readily establish Theorem 2. Again, exploiting linearity we partition $\hat{x}_m[n]$ into two components: $\hat{x}_m^{(1)}[n]$, which is generated by the set of transmitted sequences $x_i[n]$, and $\hat{x}_m^{(2)}[n]$, which is generated by the background noise $w[n]$.

When in Proposition 1 we let $p_i[n] = x_i[n]$ and $f_{ij}[n;\, k] = c_{ij}[n;\, k]$, we readily obtain, using superposition, that

$$\hat{x}_m^{(1)}[n] = \sum_{i=1}^{M} q_{im}[n] \overset{\text{m.s.}}{\to} E[C_{mm}]x_m[n] + v_m^{(1)}[n] \tag{127}$$

where

$$v_m^{(1)}[n] = \sum_{i=1}^{M} z_{im}[n].$$

Note, in addition, that due to the properties of the $z_{ij}[n]$ in Proposition 1, the $v_m^{(1)}[n]$ are mutually uncorrelated, zero-mean, white marginally Gaussian noise sequences with variances

$$\operatorname{var} v_m^{(1)}[n] = \frac{1}{M}\sum_{i=1}^{M} \mathcal{E}_i \operatorname{var}[C_{im}]. \tag{128}$$

Next, when in Proposition 1 we let

$$p_i[n] = \sum_k w[k]h_m[k - nM] \quad \text{and} \quad f_{ij}[n;\, k] = b_j[n;\, k]$$

we again readily obtain that

$$\hat{x}_m^{(2)}[n] = \sum_{i=1}^{M} q_{im}[n] \overset{\text{m.s.}}{\to} v_m^{(2)}[n] \tag{129}$$

where the $v_m^{(2)}[n]$ are mutually uncorrelated, zero-mean, white marginally Gaussian noise sequences with variances

$$\begin{aligned} \operatorname{var} v_m^{(2)}[n] &= \mathcal{N}_0\mathcal{W}_0|E[B_m]|^2 + \mathcal{N}_0\mathcal{W}_0 \operatorname{var}[B_m] \\ &= \mathcal{N}_0\mathcal{W}_0 E[|B_m|^2]. \end{aligned} \tag{130}$$

Hence, combining (127) and (129) we obtain (56) where

$$v_m[n] = v_m^{(1)}[n] + v_m^{(2)}[n].$$

Furthermore, since the $x_m[n]$ and $w[n]$ are uncorrelated, we obtain (57) using

$$\operatorname{var} v_m[n] = \operatorname{var} v_m^{(1)}[n] + \operatorname{var} v_m^{(2)}[n]$$

with (128) and (130).

Appendix IV
Proof of Lemma 1

First, note we may rewrite (59) in the form

$$\gamma_m(B) = \frac{\mathcal{E}_m|E[A_m B]|^2}{E[|\xi B|^2] - \frac{1}{M}\sum_k \mathcal{E}_k|E[A_k B]|^2} \tag{131}$$

where

$$\xi = \sqrt{\mathcal{N}_0\mathcal{W}_0 + \frac{1}{M}\sum_k \mathcal{E}_k|A_k|^2}. \tag{132}$$

Using the invertible change of variables

$$\tilde{B} = B^*\xi \tag{133}$$

$$\tilde{A}_m = \sqrt{\mathcal{E}_m}A_m/\xi \tag{134}$$

we can then rewrite (131) in the form

$$\gamma_m(\tilde{B}) = \frac{|E[\tilde{B}^*\tilde{A}_m]|^2}{E[|\tilde{B}|^2] - \frac{1}{M}\sum_k |E[\tilde{B}^*\tilde{A}_k]|^2}. \tag{135}$$

Note that by symmetry, $\tilde{A}_1, \tilde{A}_2, \cdots, \tilde{A}_M$ are also zero-mean, mutually uncorrelated random variables, whose variances we denote by $\lambda_1, \lambda_2, \cdots, \lambda_M$.

Now, any $\tilde{B}$ with finite variance can be expanded in the form

$$\tilde{B} = \epsilon + \sum_{k=1}^{M} \eta_k \tilde{A}_k \tag{136}$$

where, for all k, $E[\epsilon^* A_k] = 0$ and η_k are complex constants. In particular, it suffices to choose

$$\eta_k = E[B^*\tilde{A}_k]/E[|\tilde{A}_k|^2].$$

Furthermore, from (59) we see that if $\hat{B}$ maximizes γ_m, so does $\kappa\hat{B}$ for any κ. Hence, to fix a particular solution, we may, without loss of generality, set $\eta_m = 1$.

Using (136), (135) simplifies to

$$\gamma_m(\tilde{B}) = \gamma_m^2 \left(E[|\epsilon|^2] + \lambda_m(1 - \lambda_m/M) + \sum_{k\neq m} |\eta_k|^2 \lambda_k(1 - \lambda_k/M), \right)^{-1}$$

which, since

$$\lambda_i = E\left[\frac{\mathcal{E}_i|A_i|^2}{N_0 + \frac{1}{M}\sum_k \mathcal{E}_k|A_k|^2}\right] \leq M$$

is maximized when $\epsilon = 0$ and $\eta_k = 0$ for $k \neq m$. Thus the maximum value of γ_m is obtained when B is of the form (60).

To obtain the bound (62), it suffices to substitute the optimum value of b into (131), which yields

$$\gamma_m/M = \frac{\varphi_m/M}{1 - \varphi_m/M} = \frac{1}{1 - \varphi_m/M} - 1$$

where

$$\varphi_m = E[\mathcal{E}_m|A_m|^2/\xi^2].$$

It, therefore, remains only to note that

$$1 - \varphi_m/M = E\left[\frac{\mathcal{N}_0\mathcal{W}_0 + \frac{1}{M}\sum_{k\neq m} \mathcal{E}_k|A_k|^2}{\mathcal{N}_0\mathcal{W}_0 + \frac{1}{M}\sum_k \mathcal{E}_k|A_k|^2}\right].$$

APPENDIX V
PROOF OF LEMMA 2

Let ξ_m denote the left-hand side of (68). Then

$$\xi_1 = \xi_2 = \cdots = \xi_M \triangleq \xi_0$$

and, hence

$$\begin{aligned}\xi_0 &= \frac{1}{M} E\left[\sum_k v_k\right] \\ &= \frac{1}{M} E\left[\frac{M + (M-1)\sum_k v_k}{1 + \sum_k v_k}\right] \\ &= \frac{M-1}{M} + \frac{1}{M}\varphi \end{aligned} \tag{137}$$

where

$$\varphi = E\left[\frac{1}{1+\overline{\gamma}}\right] \tag{138}$$

with

$$\overline{\gamma} = \sum_k v_k. \tag{139}$$

Now $\overline{\gamma}$ as defined in (139) is an Erlang random variable of order M and mean M/μ. Hence

$$\varphi = \int_0^\infty \frac{\mu^M \overline{\gamma}^{M-1} e^{-\mu\overline{\gamma}}}{(1+\overline{\gamma})(M-1)!}\, d\overline{\gamma}. \tag{140}$$

Exploiting the identities [19]

$$\int_0^\infty \frac{e^{-st}}{1+t}\, dt = e^s E_1(s)$$

$$\int_0^\infty t^k e^{-st}\, dt = k!/s^{k+1}$$

and

$$\frac{t^n}{t+1} = \frac{(-1)^n}{t+1} + \sum_{k=0}^{k-1} (-1)^{n-k-1} t^k$$

we get

$$\varphi = \frac{\mu^M}{(M-1)!}\left[(-1)^{M+1} e^\mu E_1(\mu) + \sum_{k=0}^{M-2} (-1)^{M-k} k!/\mu^{k+1}\right]. \tag{141}$$

Finally, substituting (141) into (137) we get (68). ■

ACKNOWLEDGMENT

The author wishes to thank N. S. Jayant, C-E. Sundberg, N. Seshadri, J. Kovacevic, M. Sondhi, A. Odlyzko, E. Teletar, A. Wyner, and S. Shamai (Shitz), all at AT&T Bell Laboratories, for many helpful discussions, comments, and suggestions regarding this work. He also wishes to thank the anonymous reviewers for their careful reading of the manuscript and thoughtful feedback.

REFERENCES

[1] G. W. Wornell, "Spread-response precoding for communication over fading channels," *IEEE Trans. Inform. Theory,* accepted for publication.
[2] A. J. Viterbi, "Wireless digital communication: A view based on three lessons learned," *IEEE Commun. Mag.*, vol. 29, pp. 33–36, Sept. 1991.
[3] P. P. Vaidyanathan, *Multirate Systems and Filter Banks.* Englewood Cliffs, NJ: Prentice-Hall, 1993.
[4] H. L. Van Trees, *Detection Estimation, and Modulation Theory, Part I.* New York: Wiley, 1968.
[5] L. R. Welch, "Lower bounds on the maximum cross correlation of signals," *IEEE Trans. Inform. Theory,* vol. IT-20, pp. 397–399, May 1974.
[6] D. V. Sarwate and M. B. Pursley, "Crosscorrelation properties of pseudorandom and related sequences," *Proc. IEEE,* vol. 68, pp. 593–619, May 1980.
[7] M. J. E. Golay, "A class of finite binary sequences with alternate autocorrelation values equal to zero," *IEEE Trans. Inform. Theory,* vol. IT-18, no. 3, pp. 449–450, 1972.
[8] M. J. E. Golay, "Multislit spectrometry," *J. Opt. Soc. Amer.,* vol. 39, pp. 437–444, 1949.
[9] ——, "Static multislit spectrometry and its application to the panoramic display of infrared spectra," *J. Opt. Soc. Amer.,* vol. 41, pp. 468–472, 1951.
[10] ——, "Complementary series," *IRE Trans. Inform. Theory,* vol. IT-7, pp. 82–87, Apr. 1961.
[11] S. Eliahou, M. Kervaire, and B. Saffari, "On Golay polynomial pairs," *Adv. Appl. Math.,* vol. 12, pp. 235–292, 1991.
[12] R. Turyn, "Ambiguity functions of complementary sequences," *IEEE Trans. Inform. Theory,* vol. IT-9, pp. 46–47, Jan. 1963.
[13] Y. Taki, H. Miyakawa, M. Hatori, and S. Namba, "Even-shift orthogonal sequences," *IEEE Trans. Inform. Theory,* vol. IT-15, pp. 295–300, Mar. 1969.
[14] C.-C. Tseng and C. L. Liu, "Complementary sets of sequences," *IEEE Trans. Inform. Theory,* vol. IT-18, pp. 644–652, Sept. 1972.
[15] H. S. Shapiro, "Extremal problems for polynomials and power series," Master's thesis, MIT, Cambridge, MA, 1951.
[16] W. Rudin, "Some theorems on Fourier coefficients," *Proc. Amer. Math. Soc.,* vol. 10, pp. 855–859, 1959.
[17] A. M. Odlyzko, "Extremal and statistical properties of trigonometric polynomials with ± 1 and 0, 1 coefficients," preprint, 1993.
[18] D. J. Newman and J. S. Byrnes, "The L^4 norm of a polynomial with coefficients ± 1," *Amer. Math. Monthly,* vol. 97, pp. 42–45, 1990.
[19] M. Abramowitz and I. A. Stegun, Eds., *Handbook of Mathematical Functions.* New York: Dover, 1965.
[20] S. Verdú, "Minimum probability of error for asynchronous Gaussian multiple-access channels," *IEEE Trans. Inform. Theory,* vol. IT-32, pp. 85–96, Jan. 1986.
[21] ——, "Optimum multiuser asymptotic efficiency," *IEEE Trans. Commun.,* vol. COM-34, pp. 890–897, Sept. 1986.